Published in final edited form as:
*J Comp Neurol*. 2014 August 1; 522(11): 2532–2552. doi:10.1002/cne.23548.

# Localization of Tyrosine Hydroxylase-like Immunoreactivity in the Nervous Systems of *Biomphalaria glabrata* and *Biomphalaria alexandrina*, Intermediate Hosts for Schistosomiasis

**Deborah Vallejo**[1], **Mohammed R. Habib**[2,3], **Nadia Delgado**[1], **Lee O. Vaasjo**[1], **Roger P. Croll**[2], and **Mark W. Miller**[1,*]

[1]Institute of Neurobiology and Department of Anatomy & Neurobiology, University of Puerto Rico, Medical Sciences Campus, 201 Blvd del Valle, San Juan, Puerto Rico 00901

[2]Department of Physiology and Biophysics, Dalhousie University, Halifax, Nova Scotia B3H 1X5, Canada

[3]Theodor Bilharz Research Institute, Giza, Egypt

## Abstract

Planorbid snails of the genus *Biomphalaria* are major intermediate hosts for the digenetic trematode parasite *Schistosoma mansoni*. Evidence suggests that levels of the neurotransmitter dopamine (DA) are reduced during the course of *S. mansoni* multiplication and transformation within the snail. This investigation used immunohistochemical methods to localize tyrosine hydroxylase (TH), the rate-limiting enzyme in the biosynthesis of catecholamines, in the nervous system of *Biomphalaria*. The two species examined, *Biomphalaria glabrata* and *Biomphalaria alexandrina*, are the major intermediate hosts for *S. mansoni* in sub-Saharan Africa, where more than 90% of global cases of human intestinal schistosomiasis occur. TH-like immunoreactive (THli) neurons were distributed throughout the central nervous system (CNS) and labeled fibers were present in all commissures, connectives, and nerves. Some asymmetries were observed, including a large distinctive neuron (LPeD1) in the pedal ganglion described previously in several pulmonates. The majority of TH-like immunoreactive neurons were detected in the peripheral nervous system (PNS), especially in lip and foot regions of the anterior integument. Independent observations supporting the dopaminergic phenotype of THli neurons included 1) block of LPeD1 synaptic signaling by the D2/3 antagonist sulpiride, and 2) the similar localization of aqueous aldehyde (FaGlu) induced fluorescence. The distribution of THli neurons indicates that, as in other gastropods, dopamine functions as a sensory neurotransmitter and in the regulation of feeding and reproductive behaviors in *Biomphalaria*. It is hypothesized that infection could stimulate

*Address for correspondence: Dr. Mark W. Miller, Institute of Neurobiology, University of Puerto Rico, 201 Blvd del Valle, San Juan, Puerto Rico 00901, Tel: (787) 721-4149, Fax: (787) 725-3804, mark.miller@upr.edu.

**Role of Authors.** All authors had full access to all the data in the study and take responsibility for the integrity of the data and the accuracy of the data analysis. Study concept and design: RPC and MWM. Acquisition of data: DV, MRH, ND, LOV. Analysis and interpretation of data: MRH, RPC, MWM. Drafting of the manuscript: MRH, RPC, MWM. Critical revision of the manuscript for important intellectual content: MRH, RPC, MWM. Obtained funding: MRH, RPC, MWM. Administrative, technical, and material support: ND. Study supervision: RPC, MWM.

**Conflict of interest statement.** The authors have no known or potential conflict of interest including any financial, personal or other relationships with other people or organizations within three years of beginning the submitted work that could inappropriately influence, or be perceived to influence, their work.

transmitter release from dopaminergic sensory neurons and that dopaminergic signaling could contribute to modifications of both host and parasite behavior.

**Keywords**

*Schistosoma mansoni*; dopamine; pulmonate mollusk; pond snail; trematode

## INTRODUCTION

The parasitic disease schistosomiasis (snail fever) is estimated to impact seventy-seven developing countries, where its socioeconomic toll is second only to malaria (World Health Organization Media Centre 2012; Hotez 2008; King 2010). The trematode species *Schistosoma mansoni* that causes the most widespread form of intestinal schistosomiasis utilizes the planorbid snail *Biomphalaria* as its major intermediate host (Rollinson and Chappell 2002; Bayne 2009; Toledo and Fried 2010). *Biomphalaria glabrata* and *Biomphalaria alexandrina* are the principal intermediate hosts for *S. mansoni* in sub-Saharan Africa, where approximately 90% of the global cases occur. Within the gastropod host, schistosome larvae undergo multiplication and transformation into cercariae that are capable of infecting humans.

Survival and propagation of trematode larvae within the snail both depend upon complex bidirectional signaling between host and parasite (de Jong-Brink et al. 2001; Yoshino et al. 2001). Specific neurotransmitters that are shared by both schistosomes and gastropods, such as the biogenic amine dopamine (DA; 3,4-dihydroxyphenethylamine), are leading candidates for host-parasite communication, as both species possess the requisite synthetic enzymes, receptors, and uptake mechanisms necessary to achieve such signaling (Hamdan and Ribeiro 1998; Taman and Ribeiro 2009; Larsen et al. 2011).

Dopamine is a major neurotransmitter in the gastropod central nervous system (CNS) where it can produce both excitatory and inhibitory synaptic actions (Sweeney 1963; Carpenter et al. 1971; Osborne and Cottrell 1971; Ascher 1972; Berry and Cottrell 1973; McCaman et al. 1973). The presence of DA in *B. glabrata* was originally examined using spectrofluorometric measurements and its localization within the nervous system was demonstrated with histochemical fluorescence microscopy (Chiang et al. 1974). Significant reductions in DA content were measured in the *Biomphalaria* CNS during the course of *S. mansoni* infection (Manger et al. 1996). Recently, a DA transporter (SmDAT) was shown to be expressed at high levels in the parasitic stages of *S. mansoni* and it was proposed that the larval trematode could reduce its metabolic costs by scavenging DA from its host (Larsen et al. 2011). To date, however, potential neural sources of DA in *Biomphalaria* and the stimuli that could promote its release and availability to parasites have not been identified.

Histological findings indicate that DA also participates in sensory signaling by the peripheral nervous system (PNS) of gastropods (Osborne and Cottrell 1971; Croll 2001; Faller et al. 2008). While the modality of peripheral dopaminergic neurons remains uncertain, they are generally associated with cephalic sensory organs (CSOs) that mediate contact chemoreception and mechanoreception (Salimova et al. 1987; Croll et al. 2003;

Wyeth and Croll 2011). Peripheral dopaminergic neurons project to the CNS where their synaptic actions can influence the expression of behavior (Nargeot et al. 1999; Martínez-Rubio et al. 2009; Wyeth and Croll 2011; Bédécarrats et al. 2013).

In addition to mediating rapid synaptic signaling, dopamine exerts widespread modulatory actions that can regulate entire neural circuits in the gastropod CNS (Wieland and Gelperin 1983; Trimble and Barker 1984; Kyriakides and McCrohan 1989; Kabotyanski et al. 2000). Such dopaminergic modulation has been intensively studied in the central networks that control feeding, where specific dopaminergic neurons exert broad and coordinated influence over the central pattern generator (CPG) networks that control consummatory actions (Rosen et al. 1991; Teyke et al. 1993; Quinlan et al. 1997; Kabotyanski et al. 1998; Narusuye and Nagahama 2002). The ability of these interneurons to implement qualitative and quantitative specification of feeding motor programs is attributable to their capacity to reconfigure multifunctional CPG networks (Kupfermann and Weiss 2001; Murphy 2001; Cropper et al. 2004). It has been proposed that such features of motor system control can provide opportunities for parasites to alter host behavior (see de Jong-Brink et al. 1999; Katz and Edwards 1999; Adamo 2002, 2005).

In this study, immunohistochemical methods were used to localize tyrosine hydroxylase, the rate-limiting enzyme in catecholamine biosynthesis (see Osborne et al. 1975, 1976; Osborne 1977), in the central nervous system and cephalopedal sensory organs of *Biomphalaria glabrata* and *Biomphalaria alexandrina*. Emphasis was placed on identification of catecholaminergic neurons that could serve as 1) sources of host-derived DA in the developmental and reproductive program of *S. mansoni*, and 2) potential targets for parasite-induced modification of snail behavior. Preliminary reports of these observations were presented in abstract form (Delgado et al. 2010; Vallejo et al. 2011).

## MATERIALS AND METHODS

### Specimens, dissections, and nomenclature

Experiments were conducted on *Biomphalaria glabrata* that were reared in the laboratory in Puerto Rico and *Biomphalaria alexandrina* that were collected from water courses in Giza governorate, Egypt. The latter snails were held for six weeks in the Medical Malacology Laboratory, Theodor Bilharz Research Institute, Egypt, and examined on a weekly basis for natural infections before being shipped to Nova Scotia. All snails in the laboratory colonies were housed in glass or plastic aquaria at room temperature (21 – 25° C) and fed carrots or lettuce *ad lib*. Tanks contained distilled water with Instant Ocean (Kingman AZ) added (1 g per gallon) to approximate pond water and crushed oyster shells or blackboard chalk as calcium supplements. Snails dissected at 6-10 mm shell diameter were considered to be sexually mature, as evidenced by their capacity to lay eggs. Protocols conducted on *B. glabrata* were approved by the Institutional Animal Care and Use Committee (IACUC) of the University of Puerto Rico Medical Sciences Campus (Protocol #3220110). Protocols conducted on *B. alexandrina* were approved by the Animal Care Committee of Dalhousie University (Protocol #I13-06).

General features of the *Biomphalaria* nervous system have been reported previously (Lever et al. 1965; Chiang et al. 1972, 1974; Delgado et al. 2012). In the present study, a 'head-brain' preparation was developed to facilitate visualizing relations between central and peripheral cephalic structures (Fig. 1). In this dissection, the body walls were reflected and pinned laterally following a longitudinal incision of the dorsal midline integument. An effort was made to maintain the innervation of the foot, lips, and tentacles as close as possible to its natural conformation. In most preparations, the reproductive and digestive systems were removed, and the buccal ganglion was freed from the buccal mass by severing its peripheral nerves.

In preparations of the isolated nervous system and in nerve backfill experiments (below), two manipulations were implemented to obtain a planar configuration of the circumesophageal ring ganglia (see Delgado et al. 2012). For experiments in which the cerebral hemiganglia remained paired, the pedal commissure was severed and the pedal ganglia were rotated laterally (Figs. 2 - 5). In other experiments (Figs. 7 - 8), the cerebral commissure was severed, and the cerebral hemiganglia were reflected to expose the dorsal surface of the paired pedal ganglia. These midline sections were performed following the backfill procedure to preserve visualization of contralateral neurons labeled via commissural projections.

Nerve designations followed previous reports (Pan 1958; Lever et al. 1965; Chiang et al. 1972, 1974). The 'foot-brain' preparation confirmed earlier descriptions of CSO innervation, i.e. the nerve projecting to the superior lip (superior lip n.) originates medial to the nerve innervating the median lip (median lip n.) in the anterolateral cerebral ganglion (Lever et al. 1965). The two nerves cross in the periphery, taking tortuous routes to their targets (Fig. 1B). The nomenclature adopted for the pedal nerves followed Chiang et al. (1972) with the designations of anterior pedal nerve, central pedal nerve, and posterior pedal nerve corresponding respectively to nerves 10, 11, 12 used previously (Delgado et al. 2012; see Kemenes et al. 1989). Neuron cluster labels followed common usage in the intensively studied pulmonate, *Lymnaea stagnalis* (Slade et al. 1981; Benjamin and Winlow 1981; Croll and Chiasson 1990; Kemenes et al. 1989). As *Lymnaea* is a dextral species, the nomenclature used previously for the sinistral *Helisoma trivolvis* (Syed et al. 1993; Kiehn et al. 2001) was adopted when applicable (see Delgado et al. 2012).

## Wholemount immunohistochemistry

Specimens were dissected in snail saline with the following composition (in mmol $l^{-1}$): NaCl 51.3, KCl 1.7, $MgCl_2$ 1.5, $CaCl_2$ 4.1, HEPES 5, pH 7.8. Tissues were fixed for 30 m in cold methanol 99%, glacial acetic acid 1%. Following fixation, tissues were washed (5 × 20 min) in in 80 mM phosphate buffer containing 2% Triton X-100 and 0.1% sodium azide (solution referred to below as PTA).

Following preincubation with normal goat serum (0.8% in PTA, 3-5 hr, room temperature), tissues were immersed (1 – 7 days, 4° C) in a mouse monoclonal antibody (ImmunoStar, Stillwater MN; Product No. 22941; *JCN* Antibody Data Base entries 5523-5529; NIH Neuroscience Information Framework Antibody Registry Identification Number: AB_572268) generated against rat tyrosine hydroxylase (lot LNC1 purified from rat

pheochromocytoma [PC12] cells). Primary antibody concentrations ranged from 1:100 to 1:300 (see Díaz-Ríos et al. 2002; Martínez-Rubio et al. 2009). This antibody possesses wide species cross-reactivity, which is proposed to reflect its recognition of a highly conserved epitope in the mid-portion of the TH molecule (ImmunoStar Specification Sheet 22914). It specifically labels neurons that are stained using several independent techniques for catecholamines, including the glyoxylic acid (Rathouz and Kirk 1988; Elekes et al. 1991; Kabotyanski et al. 1998) and the formaldehyde (Fa) – glutaraldehyde (Glu) histofluorescence techniques (Quinlan et al. 1997; Croll 2001; Díaz-Ríos et al. 2002). Additional biochemical and pharmacological studies indicate that DA is the major catecholamine neurotransmitter in gastropods (Carpenter et al. 1971; McCaman et al. 1973, 1979; Osborne et al. 1975; Trimble et al. 1984), and that DA mediates synaptic signaling by neurons labeled with this antibody (Teyke et al. 1993; Magoski et al. 1995; Quinlan et al. 1997; Díaz-Ríos and Miller 2005). Collectively, these observations support the utility of this antibody for labeling gastropod neurons with a dopaminergic phenotype.

Following repeated PTA washes (5 times, at least 30 min each, room temperature), ganglia were incubated in secondary antibodies conjugated to fluorescent markers (Alexa 488 goat anti-mouse IgG (H+L) conjugate or Alexa 546 goat anti-mouse IgG (H+L); Molecular Probes). Secondary antibody dilutions ranged from 1:1,000 to 1:600 and incubation times ranged from 2 to 10 days. Control experiments in which either the primary or secondary antibodies were omitted resulted in the elimination of labeling.

Processed tissues were initially examined and photographed on a Nikon Eclipse or Leica DM 4000B fluorescence microscope. Imaging of favorable preparations was performed on a Zeiss Laser Scanning Confocal Microscope (Pascal LSCM) or on a Zeiss LSM 510 (META). Stacks of optical sections (0.2 - 1.5 μm) were collected to generate maximum intensity projections. Confocal images were captured in the Zeiss LSM 5 Image Browser (Version 3.1.0.11) or Zen programs of the META. Stacks, z-series, overlays, and calibrations were generated using ImageJ software (v. 1.43u, NIH public domain). Images were imported to CorelDraw 10 or Microsoft PowerPoint v. 14.0.0 files for addition of labels, adjustment of brightness / contrast, and organization of panels.

### Formaldehyde–glutaraldehyde histochemical staining

The localization of catecholamines in the nervous system of *Biomphalaria* was substantiated with the formaldehyde–glutaraldehyde (FaGlu) method of Furness et al. (1977), as modified by Croll and Chiasson (1990) for wholemount molluscan tissues. Briefly, dissected ganglia and peripheral tissues were fixed overnight at 4°C in a solution of 4% paraformaldehyde and 0.5% glutaraldehyde (Electron Microscopy Sciences, 16320) in 0.1 M PBS adjusted to pH 7.4. The tissues were then rinsed twice in 0.1 M PBS, air dried overnight (Hauser and Koopowitz 1987), and mounted between glass cover slips in a 3:1 solution of glycerol to 0.1 M Tris buffer (pH 8.0) with the addition of 2% n-propyl gallate for imaging using the Leica DM 4000B microscope. Blue-green fluorescence under UV illumination was indicative of catecholamines, as reported in other gastropods (Quinlan et al. 1997; Croll 2001; Díaz-Ríos et al. 2002). Control tissues fixed without glutaraldehyde exhibited no corresponding fluorescence.

### Nerve backfills

Dissection protocols were performed as described above. Dissected ganglia were positioned with minutien pins near a small petroleum jelly (Vaseline) enclosure (3-5 mm diameter) on the surface of a Sylgard-lined Petri dish. The nerve of interest was cut and its end was drawn into the Vaseline-lined pool. The saline was withdrawn from the pool and replaced with a saturated solution (1.4 mg / 50 μl $dH_2O$) of biocytin (Sigma-Aldrich, St. Louis, MO). The enclosure was sealed with Vaseline and the preparation was incubated overnight at room temperature to allow migration of the biocytin. The nerve was then extracted from the pool and the ganglia were repinned and washed 3-5 times with saline. Following fixation in 4% paraformaldehyde (see Díaz-Ríos et al. 2002), tissues were transferred to microcentrifuge tubes, washed 5 times (30 min each) with PTA solution and incubated in Alexa Avidin 488 (Molecular Probes, Eugene, OR) diluted 1:1,000 to 1:2,000 in PTA (24-48 h, room temperature). The preparations were assessed daily (one to five days) until the quality of the backfill staining was determined to be sufficient for advancing to immunohistochemical processing.

### Electrophysiology

Ganglia were pinned to a Sylgard-lined chamber and exposed to protease (Sigma Type XIV, 1.2 mg/ml, 15-20 m) dissolved snail saline to facilitate electrode penetration through the external sheath. Microelectrode tips were filled with 4% Neurobiotin (Vector Laboratories, Burlingame CA) dissolved in 0.5 M KCl, and 50 mM Tris (pH 7.6). The shaft of the pipette contained 2 M KCl resulting in electrode resistances ranging from 30 to 50 MΩ Following cell identification, the snail saline was replaced with a high-$Ca^{2+}$/high-$Mg^{2+}$ solution (NaCl 51.3 mM, KCl 1.7 mM, $MgCl_2$ 1.5 mM, $CaCl_2$ 24.6 mM, $MgCl_2$, 9 mM, HEPES 5 mM, pH 7.8) to attenuate polysynaptic activity (Syed et al., 1993; Magoski and Bulloch 1999). (±)-Sulpiride (Sigma-Aldrich, S8010) was dissolved in the high-$Ca^{2+}$/ high-$Mg^{2+}$ saline prior to superfusion.

### Neuron labeling

Depolarizing current pulses (1 - 2 nA; 0.5 sec; 1 Hz; 30 - 60 minutes) were used to eject the Neurobiotin from the pipette tips. Preparations were incubated overnight (4° C) to allow injected material to diffuse from the cell body to small and distant processes. Ganglia were then repinned and fixed as described above. The fixed ganglia were transferred to microcentrifuge tubes and washed five times (30 min each) with PTA solution. They were then incubated in Alexa Streptavidin 546 (Molecular Probes) diluted (1:800 to 1:3,000) in PTA (24 - 48 hrs, room temperature). Tissues were washed five times with PTA and viewed on the Nikon Eclipse TE200 fluorescence microscope prior to immunohistochemistry processing.

## RESULTS

THli neurons were widely distributed throughout the CNS and immunoreactive fibers were present in all major connectives and commissures of both *B. glabrata* and *B. alexandrina*. While the patterns of THli were highly similar between the two species, some differences were observed in the positions and occurrence of specific cells and clusters. In addition to

the central THli neurons, thousands of subepithelial sensory neurons were present in the body wall of both species. The patterns of FaGlu staining in both the CNS and PNS were consistent with the localization of THli, supporting the hypothesis that these cells contain catecholamines.

## Cerebral ganglion

THli neurons were present on the dorsal and ventral aspects of the cerebral ganglion (Figs. 2 - 4). Most of the THli neurons visible from the dorsal surface of the cerebral ganglia were proximate to the base of the tentacular nerve (T n., Fig. 2A-C). Four to six moderately sized (15-20 μm) cells positioned near each tentacular nerve gave rise to processes oriented in the medial direction toward the origin of the tentacular nerve fiber tract (e.g. Fig. 2A-C). A compact cluster of ten to twelve smaller (10-15 μm) neurons was positioned anteromedial to the tentacular nerve, approximately 50 μm below the dorsal surface (Fig. 2A, B). The cells comprising this cluster were oriented in a posterolateral direction and their axons converged to project in the direction of the tentacular nerve.

TH-like staining was present in two bilateral structures corresponding to the medio-dorsal bodies (MDB) and latero-dorsal bodies (LDB) described initially in *Lymnaea stagnalis* by Joosse (1964; Fig. 2A, D, E). The MDB (Fig. 2A, D) adhered to the cerebral commissure and the LDB (Fig. 2A, E) protruded from the posterior edge of each hemiganglion. In both dorsal bodies, staining was observed in small (4-6 μm diameter) densely packed cells with large prominent nuclei (Fig. 2D, E).

The majority of THli neurons on the ventral surface of the cerebral ganglion were located near the confluence of the lip nerves and the cerebral commissure (Fig. 3A-C). These neurons exhibited a range of sizes (10-20 μm), shapes, and staining intensities (Fig. 3B, C). Two brightly stained cells were distinguished on the surface of the cerebral ganglia in both *B. glabrata* and *B. alexandrina*. Prominent axons projected from these cells in the lateral direction (Fig. 3 B, C, arrows). In both species, a group of five or six less intensely stained somata was located 10 to 20 μm below the surface (Fig. 3 B, C, arrowheads).

The cerebral commissure (Fig. 3A, C c.) contained numerous immunoreactive fibers, some of which formed a compact fascicle (Fig. 3D). The only unpaired THli neurons detected in the cerebral ganglia formed a cluster of 6 to 8 small (soma diameter 10-15 μm) cells near the ventral surface of the right cerebral hemiganglion (Fig. 3D). The axons of these cells converged and projected toward the posterior cerebral commissure. The remaining ventral THli neurons were present in the lateral region of the cerebral ganglia near the origin of the medial lip nerve and cerebral-buccal connective (Fig. 3E, F). These cells exhibited a range of sizes (10 – 30 μm) and staining intensities. In some preparations, fibers from this cluster could be seen to enter the cerebral-buccal connective (see Fig. 4). A prominent bipolar neuron protruded from the lateral edge of the medial lip nerve, giving rise to axons that joined this nerve in both the centripetal and centrifugal directions (Fig. 3 E, F).

Major THli fiber projections were present in the tentacular nerve (Fig. 2A) and in the superior and medial lip nerves (Fig. 4A). In preparations where the nervous system remained connected to the lips and tentacles (see Fig. 1A), the lip nerves projected to a population of

distal THli neurons (Fig. 4A, B). The peripheral THli cell bodies (6-8 μm in diameter) lined the lips, projecting apical processes (20 – 30 μm) through the epithelium toward the surface (Fig. 4B). They did not extend beyond the epithelial surface where they terminated in a bulbous swelling (Fig. 4C). Longer proximal processes converged in branches of the lip nerves projecting toward the CNS. When the lips were viewed from the exterior surface, the distal processes of the THli cells were observed to fully penetrate the epithelium of the superior and inferior lip regions (Fig. 4D).

## Buccal ganglion

THli neurons were present on the caudal and rostral surfaces of the buccal ganglion (Fig. 5). Caudal cells included a pair of lateral neurons positioned near the confluence of the esophageal nerve and the cerebral-buccal connective of each hemiganglion (Fig. 5A, C, D). In both *B. glabrata* and *B. alexandrina* these neurons gave rise to axons projecting toward the buccal commissure (Fig. 5C, D, arrows). In addition to these bilateral neurons, an unpaired immunoreactive neuron was present near the buccal commissure on the caudal surface of the right hemiganglion (Fig. 5A, arrow). Smaller (5-10 μm) neurons exhibiting weaker immunoreactivity were distributed throughout the buccal ganglion. On the rostral surface, a pair of moderately sized (15-20 μm) strongly staining cells flanked the buccal commissure (Fig. 5B, arrows) and additional small cells were observed. Prominent THli fiber tracts were present in the buccal commissure, the esophageal trunk, and the cerebral-buccal connective.

The presence of THli fibers in the cerebral-buccal connective (Fig. 5A) prompted experiments using double-labeling (biocytin backfills combined with TH immunohistochemistry) to localize catecholaminergic projection neurons in the cerebral ganglia that could participate in the regulation of feeding motor patterns (see Rosen et al. 1991, Narusuye and Nagahama 2002). Most of the neurons labeled with cerebral-buccal connective backfills were located in the anterior quadrant of the ipsilateral cerebral hemiganglion (Fig. 6A; see also Delgado et al. 2012). These included the large C1 neuron (Fig. 6A), shown previously to contain serotonin-like immunoreactivity (Delgado et al. 2012). Subsequent processing for THli demonstrated double labeling in a small (15-20 μm) neuron near the origin of the cerebral-buccal connective lateral to the medial lip nerve (Fig. 6B-F). No additional double-labeled neurons were detected.

## Pedal ganglion

The most distinctive TH-like immunoreactive neuron in the CNS was located on the posterior margin of the left pedal ganglion (Fig. 7A-D). The soma of this neuron ranged from 40 to 60 μm in diameter. It was positioned on the dorsal surface bordering the medial edge of the statocyst, but it was also readily viewed from the ventral aspect due to its large size, peripheral position, and intense staining (Fig. 7B). The initial segment of the major axon appeared to be lined by a lattice of fine immunoreactive fibers (Fig. 7C, arrow). The principal axon coursed in the anterolateral direction, giving rise to several finer branches prior to turning toward the pedal-pleural connective (Fig. 7C, D). All of these characteristics support the homology of this neuron with the LPeD1 cell of *Helisoma trivolvis* (Syed et al. 1993), the giant dopamine cell of *Planorbis corneus* (Pentreath et al. 1974), and the giant

dopaminergic RPeD1 neuron of *Lymnaea* (Cottrell 1977; Cottrell et al. 1979; McCaman et al. 1979; Slade et al. 1981; see Discussion).

Two additional THli neurons were present in the central region of the dorsal surface of each pedal ganglion (Fig. 7A, arrows). One of these cells was typically larger, more superficial, and more strongly stained than the other. The fibers from these neurons projected toward the pedal-pleural connective. Two clusters of smaller (10 – 15 μm) THli neurons were present in the anterolateral quadrant of each pedal ganglion, between the origins of the anterior pedal nerve and central pedal nerve (Fig. 7B, E). These clusters were composed of 6 to 8 elongated neurons and were more readily viewed from the ventral aspect of the ganglion (Fig. 7B, E). Finally, a group of 8-10 small (10-15 μm) neurons present on the medial dorsal surface of the pedal ganglion in *B. alexandrina* (Fig. 7F) was not observed in *B. glabrata*.

The central region of each pedal ganglion contained a dense fiber network and the three pedal nerves projecting to the foot were densely filled with immunoreactive fibers (Fig. 7A,B). When these nerves were followed to their peripheral terminations, small THli bipolar neurons were observed lining the pedal epithelium (Fig. 7G). These neurons had the same size (6-8 μm diameter) and anatomical characteristics as described above for the THli immunoreactive neurons in the lips (*cf*. Fig. 4).

The large size and accessibility of LPeD1 prompted electrophysiological and pharmacological experiments to further test the role of dopamine as a neurotransmitter in neurons labeled in this study. The RPeD1 neuron of *Lymnaea* and LPeD1 of *Helisoma* participate in the central pattern generator (CPG) circuit for aerial respiration (Moroz and Winlow 1992; Syed and Winlow 1991; Syed et al. 1990, 1993). In normal saline, the LPeD1 neuron of *Biomphalaria glabrata* exhibited repetitive burst activity (Fig. 8A, lower record), suggesting that it also functions in the respiratory CPG. In agreement with observations in the other species, numerous motor neurons in the posteromedial quadrant of the visceral ganglion (J cluster) were observed to fire out of phase with LPeD1 (Fig. 8A, upper record). When the saline was replaced with a high-$Ca^{2+}$/high-$Mg^{2+}$ solution to attenuate polysynaptic activity, inhibitory postsynaptic potentials (IPSPs) were observed in the visceral neuron following each LPeD1 impulse (Fig. 8B). These IPSPs occurred with a brief and constant latency following each LPeD1 spike, indicative of direct chemical synaptic transmission. When LPeD1 was fired with progressively larger depolarizing intracellular current pulses, the IPSPs became fused and exhibited summation (Fig. 8C, left panel). Addition of sulpiride (100 μM), a selective D2/D3 antagonist of dopaminergic signaling in gastropods (Magoski et al. 1995; Quinlan et al. 1997; Díaz-Ríos and Miller 2005), blocked the IPSPs elicited by LPeD1 in a reversible fashion (Fig. 8C, middle panel). Following each experiment with sulpiride ($n$ = 4), the pre- and postsynaptic neurons were filled with neurobiotin and processed for TH-like immunoreactivity (Fig. 8, D-F). These observations support the role of dopamine as a neurotransmitter in the neurons labeled in this study.

### Pleural, parietal, and visceral ganglia

In *B. glabrata*, a single immunoreactive neuron was located at the posterolateral edge of the ventral surface of the left pleural ganglion (Fig. 7B, *arrow*). This neuron was not detected in *B. alexandrina*, where the left pleural ganglion was devoid of TH-like immunoreactive cell

bodies. In both species, the left pleural ganglion and left parietal ganglion were traversed by several THli fibres, including the large axon of the LPeD1 neuron en route to the left parietal ganglion (Fig. 9A, B, see also Fig. 7B, F). One branch of the LPeD1 neuron entered the external left parietal nerve (Fig. 9A, *arrow*, B) and continued toward the periphery following its anastomosis with the anal nerve posterior to the visceral ganglion (Fig. 9A, E; see Lever et al. 1965). Additional branches of LPeD1 projected to the internal left parietal nerve (Fig. 9A, B) and to the visceral ganglion via the parietal-visceral connective (Fig. 9B).

While three small neurons were present on the dorsolateral surface of the right parietal ganglion of *B. alexandrina* (not shown) none were detected in the R Pa g. of *B. glabrata*. In both species, two cell bodies were located in the central region of the left parietal ganglion near the bifurcation of the LPeD1 fiber (Fig. 9A, C). The more superficial cell of the pair was typically larger (20 – 30 μm) and more intensively stained than the deeper cell (15 – 20 μm). Projections from both left parietal ganglion cells were oriented toward the visceral ganglion.

Two THli cell bodies were also observed near the ventral surface of the visceral ganglion, adjacent to the LPeD1 axon Fig. 9A, D). The more superficial neuron of the pair was again larger (20 – 30 μm) and more intensively stained than the deeper cell (15 – 20 μm). Multiple fibers projected from both somata (Fig. 9D, *arrows*). Axons from the larger cell projected to the intestinal and anal nerves (Fig. 7E).

### Peripheral neurons

As described above, the tentacular, lip, and pedal nerves contained large numbers of THli fibers that projected from sensory neurons in the body wall. THli axons were similarly present in all peripheral nerves innervating the integument. A few immunoreactive cell bodies were embedded within peripheral nerves, such as the esophageal trunk (not shown) and the external left parietal nerve near its juncture with the anal nerve (Fig. 9A, E). However, the vast majority of THli axons in peripheral nerves originated from sensory neurons lining the body wall in all regions of skin examined. The THli peripheral cells were especially dense on the ventral lateral surface of the mantle, ventral surface and along the entire margin of the lip, and on the dorsal medial surface of the foot (Fig. 4B-D, 7G).

### FaGlu histochemistry

FaGlu histochmistry was used as a second marker for catecholamines in the *Biomphalaria* nervous system. Neurons stained with FaGlu exhibited intense fluorescence that generally contrasted well with background, but resolution of detail was limited due to diffuse staining of fiber systems within the ganglia. The localization of FaGlu-induced blue-green fluorescence was in agreement with the distribution of the TH-like immunoreactivity. The vast majority of cells marked with FaGlu were located in the periphery where they lined the cephalic sensory organs and other regions of the integument (Fig. 10A). FaGlu-labeled peripheral sensory cells had an epithelial process, were bipolar, and were particularly dense along the edges of the lips and anterior foot, supporting their correspondence to the THli peripheral neurons. Within the CNS, two prominent neurons were located near the lateral margin of each buccal hemiganglion (Fig. 10B), groups of stained neurons were present near

the origin of the tentacular nerve (Fig. 10C, D), and the pattern of labeled neurons in the pedal ganglia was in agreement with THli (Fig. 10E, F). A notable inconsistency between the two methods was the absence of FaGlu staining in the medial dorsal body and in the lateral dorsal body.

## DISCUSSION

The localization of THli observed in the central nervous system of *Biomphalaria glabrata* and *Biomphalaria alexandrina* (summarized schematically in Fig. 11) is in overall agreement with prior reports in several pulmonates, including *Helix pomatia* (Dahl et al. 1966; Hernádi et al. 1989), *Planorbis corneus* (Marsden and Kerkut 1970), *Lymnaea stagnalis* (Audesirk 1985; Croll and Chiasson 1990; Werkman et al. 1991; Elekes et al. 1991; Sakharov et al. 1996; Croll et al. 1999), and *Helisoma duryi* (Kiehn et al. 2001). A previous study also used fluorescence spectroscopy and histochemical fluorescence microscopy to demonstrate the presence of catecholamines in the CNS of *B. glabrata* (Chiang et al. 1974).

In early studies using glyoxylic acid histofluorescence techniques, intense staining of the neuropil regions rendered localization of central catecholaminergic neurons challenging (Marsden and Kerkut 1970; Chiang et al. 1974; Audesirk 1985; see Fig. 10 of this report). These limitations were reduced with the application of immunohistochemical approaches and serial sectioning of ganglia (Croll and Chiasson 1990; Elekes et al. 1991; Werkman et al. 1991). In the present investigation, the combination of immunohistochemistry and optical sectioning of wholemount ganglia using confocal microscopy produced a localization of central catecholaminergic cell bodies that should facilitate electrophysiological and functional characterization of catecholaminergic neurons in the *Biomphalaria* CNS.

The FaGlu histochemical staining protocol provided independent support for the dopaminergic phenotype of neurons labeled for TH. Neurons that displayed THli but were not stained by the FaGlu method could utilize norepinephrine (NE) as a neurotransmitter, as low levels of NE have been detected in pulmonate nervous systems (Trimble et al. 1994; Hernadi et al. 1993; Kiehn et al. 2001). Moreover, it is possible that our methods have not disclosed the entire population of dopaminergic neurons in *Biomphalaria*, as evidence supports the presence of dopaminergic neurons that are not TH-immunoreactive in pulmonates (see Sakharov et al. 1996).

### Identified catecholaminergic neurons

Many of the individual cells and cell clusters observed in both species of *Biomphalaria* appear to have homologs in other gastropods, suggesting their conservation across this taxon. For instance, other pulmonate species have similar clusters of catechominergic cells distributed across the cerebral ganglia and near the origins of the pedal nerves (Croll 1988; Croll et al. 1999). Moreover, the anatomical features and dopaminergic phenotype of the large pedal neuron in *Biomphalaria* are indicative of homology with the giant dopamine cell (GDC) of *Planorbis corneus* (Berry and Cottrell 1973, 1975) and the left pedal dorsal 1 (LPeD1) neuron of *Helisoma trivolvis* (Syed et al. 1993; Harris and Cottrell 1995). The location of this cell in *Biomphalaria* in the left pedal ganglion, as in *Planorbis* and

*Helisoma*, reflects the sinistrality of these species. In the dextral species *Lymnaea stagnalis*, where the central ganglia are organized as a mirror image of the sinistral CNS, the dopaminergic RPeD1 neuron exhibits all of the anatomical characteristics observed in this study (Cottrell 1979; Benjamin and Winlow 1981; Syed and Winlow 1989). Maintaining consistency with the most common nomenclature in *Lymnaea* and *Helisoma*, we have adopted the designation of left pedal dorsal 1 (LPeD1) neuron for this cell in *Biomphalaria*.

The function of RPeD1 has been extensively studied in *Lymnaea*, where it acts as an influential interneuron in the central pattern generator circuit controlling aerial respiration (Winlow et al. 1981; Syed et al. 1990, 1992; Syed and Winlow 1991). Our observations, in which LPeD1 was found to produce rhythmic burst activity in the isolated CNS and to produce direct inhibition of putative motor neurons in the visceral ganglion, are consistent with such a role in *Biomphalaria*. Blockade of these IPSPs by sulpiride, a D2/3 antagonist that blocks inhibitory and excitatory dopaminergic synapses in gastropods, provides further support for the dopaminergic phenotype of TH-positive neurons labeled in this study (see Magoski et al. 1995; Quinlan et al. 1997; Due et al. 2004; Díaz-Ríos and Miller 2005).

The distribution of THli neurons in the feeding system of *Biomphalaria* suggests additional homologies to cells identified previously in other gastropods. In *Aplysia* and *Helisoma*, influential dopaminergic interneurons are located in the buccal ganglion, within the multifunctional neural circuit that controls oral behaviors (Teyke et al. 1993; Quinlan et al. 1997; Kabotyanski et al. 1998). Murphy (2001) noted physiological and structural commonalities between specific buccal neurons of the pulmonate *Helisoma* and the opisthobranch *Aplysia* and advanced the hypothesis of a “universal gastropod tripartite buccal central pattern generator” (Murphy 2001; see also Wentzell et al. 2009). Homology was proposed between dopaminergic neurons located near the lateral edge of the caudal surface of the ganglion (N1a in *Helisoma* and B65 in *Aplysia*) and between dopaminergic interneurons located near the buccal commissure (N1b of *Helisoma* and B20 of *Aplysia*). The configuration of buccal catecholaminergic neurons in *Biomphalaria* bears considerable similarity to other gastropods and should provide further opportunities to test the proposal of a universal gastropod CPG.

## Catecholamines and the control of behavior

One aim of this study was to identify catecholaminergic neurons that could participate in interactions between *Biomphalaria* and trematode parasites. For instance, the presence of THli neurons projecting from the cerebral to the buccal ganglion supports a role for DA in the regulation of feeding. Modifications of feeding behavior in infected *Biomphalaria* have been reported and attributed to altered energy requirements for cercarial production versus egg production (see following text; Meuleman 1972; and Gilbertson 1983). Application of exogenous DA evokes coordinated buccal motor patterns (BMPs) in several gastropods, including the pulmonates *Helisoma trivolvis* (Trimble and Barker 1984; Trimble et al. 1984; Quinlan et al. 1997), *Limax maximus* (Wieland and Gelperin 1983; Wieland et al. 1987), and *Lymnaea stagnalis* (Kyriakides and McCrohan 1989). In *Aplysia californica*, a bilateral pair of dopaminergic cerebral-buccal interneurons (CBIs), termed CBI-1, were shown to respond to tactile stimuli to the tentacles, lips, and buccal mass, and to evoke a BMP when fired

repetitively (Rosen et al. 1991). A pair of dopaminergic cerebral neurons (CBM1) in *Aplysia kurodai* that are proposed to be homologous to CBI-1 of *A. californica*, bias the feeding motor circuitry toward the rejection of non-preferred foods (Narusuye and Nagahama 2002). Together, the presence of THli neurons within the buccal circuit and others projecting from the cerebral ganglion support pivotal 'intrinsic' and 'extrinsic' regulatory roles for DA in the control of *Biomphalaria* feeding circuits (see Katz 1995; Katz and Frost 1996). This neural architecture affords opportunities for parasites to modify consummatory behavior by altering the activity of specific target neurons (see Katz and Edwards 1999; Adamo 2002; Lefèvre et al. 2009).

The presence of THli in the dorsal bodies suggests that DA could also be involved in the diminished egg laying, or 'parasitic castration', observed in infected snails (de Jong-Brink et al. 1995; 2001). Surgical removal of the dorsal bodies was found to significantly reduce egg production in *Lymnaea*, leading to the proposal that dorsal body endocrine cells produce a hormone (dorsal body hormone) required for female function (Geraerts and Joose 1975, Geraerts 1976). In the present study, FaGlu histofluorescence was not detected in the dorsal bodies. As this finding may reflect a lower sensitivity of the FaGlu technique, the possible role of catecholaminergic signaling in the endocrine and neural regulation of female reproductive function in *Biomphalaria* merits further study in view of findings in related pulmonates. In *Helisoma duryi*, DA was shown to stimulate secretion of perivitelline fluid from the albumen gland, a critical step for providing sufficient nutrients to the developing embryo (Saleuddin et al. 2000). THli was localized to a plexus of fibers innervating the albumen gland of *Helisoma* and it was proposed that both central and peripheral dopaminergic neurons could participate in the regulation of vitellogenin secretion (Kiehn et al. 2001).

### Catecholaminergic sensory neurons

The free swimming *S. mansoni* miracidium penetrates the cephalopedal body wall of *B. glabrata*, gaining access to the integument where it transforms into the parasitic sporocyst form (Wright 1973; Bayne 2009). Chiang et al. (1974) used fluorescence microscopy to demonstrate the presence of dopaminergic fibers in the epithelium of the mouth area, tentacles, and foot of *Biomphalaria*. Subsequent studies resolved the somata of peripheral catecholaminergic neurons in numerous gastropod species, including *Aplysia depilans* (Salimova et al. 1987), *Helix aspersa* (Hernádi and Elekes 1999), and *Lymnaea stagnalis* (Wyeth and Croll 2011). Croll (2001, 2003) demonstrated THli immunoreactive neurons in the siphon and gill epithelium of *Aplysia*, and proposed a low-threshold mechanosensory function. Faller et al. (2008) examined THli subepidermal sensory neurons in the cephalic sensory organs (CSOs: lips and tentacles) of several opisthobranchs and advanced a role for these cells in contact chemoreception or mechanoreception. Thus, while the precise sensory modality of the peripheral THli neurons of *Biomphalaria* remains to be determined, our findings demonstrate their presence in the cephalopedal epithelium, the major locus of miracidium penetration. TH-like immunoreactivity could serve as a marker for studying how infection impacts the neural innervation of the *Biomphalaria* integument.

*S. mansoni* miracidia pierce the body wall using muscular squirming and boring, aided by histolytic factors secreted by their penetration glands (Wright 1958; Maldonado 1967; Bayne 2009). Depending upon their modality, the epithelial THli neurons could respond to tactile or noxious stimuli produced by the penetrating miracidium or to one or more of its excretory-secretory products (ESPs; Lodes and Yoshino 1990; Loker et al. 1992; Yoshino et al. 2001). Moreover, the relatively large (200 μm in length) miracidium is likely to rupture receptor cells, causing release of their contents in the vicinity of the parasitic larvae. Following its entrance, the parasite typically remains close to the site of penetration, establishing intimate contact with the surrounding host tissues (Pan 1965; Wright 1973; Yoshino et al. 2001). During its transformation to the mother sporocyst stage, additional factors and larval transformation proteins (LTPs) are released (Bayne and Yoshino 1989; Yoshino et al. 1993; Wu et al. 2009). Complex molecular interactions occur with the host haemocyte defense systems during parasite penetration and transformation (de Jong-Brink et al. 2001; Humphries and Yoshino et al. 2003; Zahoor et al. 2009). The dopaminergic sensory neural innervation of the epithelium could be responsive to soluble signaling molecules generated by the parasite or host during this period of larval transformation (see de Jong-Brink 2001; Yoshino et al. 2001).

### Potential consequences of dopaminergic neuron activation

It is well established that the peripheral sensory neurons of gastropods project directly to the CNS (Jahan-Parwar 1975; Bicker et al. 1982; Nakamura et al. 1991a,b; Emery 1992; Zaitseva 1994; Xin et al. 1995). The extensive innervation of the cerebral neuropil suggests that activation of cephalic dopaminergic neurons by miracidium penetration or by factors released during parasite transformation could cause a potent and widespread release of DA at central loci. While the THli neurons of the foot project to the CNS via pedal nerves, this study does not resolve whether they terminate within the pedal ganglion or if they traverse the cerebral-pedal connective and also contribute to the cerebral neuropil. Overall, however, the distribution of THli in the CNS suggests diverse functions of dopaminergic afferents, ranging from local reflex responses to control of neural circuits and stress responses that could be expressed over multiple temporal phases of infection.

The possibility that the THli sensory neurons could also release dopamine in the periphery should be considered in view of demonstrations of somatic exocytosis and reverse transport of DA by the giant dopamine cell of *Planorbis corneus* (Chen et al. 1995; Anderson et al. 1998). Recently, a DA transporter (SmDAT) was shown to be expressed at high levels in the parasitic stages of *S. mansoni* and it was proposed that the larval trematode could reduce its metabolic costs by scavenging DA from its host (Larsen et al. 2011). Moreover, in a medium throughput screen of 1,280 small molecules for inhibition or delay of *S. mansoni* miracidial transformation *in vitro*, 12 of 47 total effective compounds were agonists or antagonists of $D_1$ or $D_2$ type dopamine receptors (Taft et al. 2010). Our findings indicate that the neural innervation of the integument could serve as one source of host-derived DA.

Finally, the observation that the apical dendrites of the peripheral THli cells penetrate the epithelium raises the possibility that DA could be released to the surrounding water. Early workers noted that the swimming miracidia are converted to an excited state when

stimulated by chemical substances emitted by snails and other organisms (Wright 1958; Etges and Decker 1963). The complex of host-derived compounds that promote miracidium orientation, host location, and locomotor behavior was designated the “miraxone” by Chernin (1970). In view of the conserved role for dopamine in regulating motor systems throughout phylogeny, we hypothesize that dopamine release from peripheral sensory neurons contributes to the *S. mansoni* miraxone.

In sum, the widespread presence of THli neurons in the peripheral nervous system of *Biomphalaria* is consistent with the participation of dopamine in multiple facets of bidirectional signaling at the snail-parasite interface (see de Jong Brink et al. 2001; Yoshino et al. 2001). Possible roles range from host location and the regulation of transformation and reproduction of the parasite, to sensory processing and the stress responses of the host. While its distribution in the central nervous system is more limited, our findings indicate that dopaminergic neurons may function as key determinants of motor control, and thus could provide effective targets for parasite-induced modifications of host behavior.

## Acknowledgments

The authors thank Drs. Fred A. Lewis, Matthew Tucker, and Matty Knight (Biomedical Research Institute) for their support.

**Support**: National Institutes of Health: RCMI RR-03051& G12-MD007600, NIGMS MBRS: GM-087200; National Science Foundation DBI-0115825 and DBI-0932955, and NHRD-1137725. Partnership and Ownership Initiative (ParOwn 0911), Ministry of High Education and Scientific Research of Egypt.

## LITERATURE CITED

Adamo SA. Modulating the modulators: parasites, neuromodulators and host behavioral change. Brain Behav Evol. 2002; 60:370–377. [PubMed: 12563169]

Anderson BB, Ewing AG, Sulzer D. Electrochemical detection of reverse transport from *Planorbis* giant dopamine neuron. Methods Enzymol. 1998; 296:675–689. [PubMed: 9779482]

Ascher P. Inhibitory and excitatory effects of dopamine on *Aplysia* neurones. J Physiol. 1972; 225:173–209. [PubMed: 4679683]

Audesirk G. Amine-containing neurons in the brain of *Lymnaea stagnalis*: distribution and effects of precursors. Comp Biochem Physiol. 1985; 81A:359–365.

Bayne CJ. Successful parasitism of vector snail *Biomphalaria glabrata* by the human blood fluke (trematode) *Schistosoma mansoni*: A 2009 assessment. Molec & Biochem Parasitol. 2009; 165:8–18. [PubMed: 19393158]

Bayne CJ, Yoshino TP. Determinants of compatibility in mollusk-trematode parasitism. Amer Zool. 1989; 29:399–407.

Bédécarrats A, Cornet C, Simmers J, Nargeot R. Implication of dopaminergic modulation in operant reward learning and the induction of compulsive-like feeding behavior in *Aplysia*. Learn Mem. 2013; 20:318–327. [PubMed: 23685764]

Benjamin PR, Winlow W. The distribution of three wide-acting synaptic inputs to identified neurons in the isolated brain of *Lymnaea stagnalis* (L.). Comp Biochem Physiol *A*. 1981; 70:293–307.

Berry MS, Cottrell GA. Dopamine: Excitatory and inhibitory transmission from a giant dopamine neurone. Nature New Biology. 1973; 242:250–253.

Berry MS, Cottrell GA. Excitatory, inhibitory and biphasic synaptic potentials mediated by an identified dopamine containing neurone. J Physiol Lond. 1975; 244:589–612. [PubMed: 1133772]

Bicker G, Davis WJ, Matera EM, Kovac MP, Stormogipson DJ. Chemoreception and mechanoreception in the gastropod mollusc *Pleurobranchaea californica*. 1. Extracellular analysis of afferent pathways. J Comp Physiol. 1982; 149:221–234.

Boer HH, Slot JW, van Andel J. Electron microscopical and histochemical observations on the relation between medio-dorsal bodies and neurosecretory cells in the Basommatophora snails *Lymnaea stagnalis*, *Ancyus fluviatilis*, *Australorbis glabratus* and *Planorbarius corneus*. Zeitschrift für Zellforschung. 1968; 87:435–450.

Boyle JP, Yoshino TP. Monoamines in the albumen gland, plasma, and central nervous system of the snail *Biomphalaria glabrata* during egg-laying. Comp Biochem Physiol A Mol Integr Physiol. 2002; 132:411–422. [PubMed: 12020657]

Central Intelligence Agency. The World Factbook 2009. Washington, DC: 2009. https://www.cia.gov/library/publications/the-world-factbook/index.html

Chen G, Gavin PF, Luo G, Ewing AG. Observation and quantitation of exocytosis from the cell body of a fully developed neuron in *Planorbis corneus*. J Neurosci. 1995; 15:7747–7755. [PubMed: 7472525]

Chernin E. Behavioral responses of miracidia of *Schistosoma mansoni* and other trematodes to substances emitted by snails. J Parasitol. 1970; 56:287–296. [PubMed: 5445826]

Chiang PK, Bourgeois JG, Bueding E. Histochemical distribution of acetylcholinesterase in the nervous system of the snail, *Biomphalaria glabrata*. Intern J Neurosci. 1972; 3:47–60.

Chiang PK, Bourgeois JG, Bueding E. 5-Hydroxytryptamine and dopamine in *Biomphalaria glabrata*. J Parasitol. 1974; 60:264–271. [PubMed: 4821112]

Cottrell GA. Identified amine-containing neurones and their synaptic connexions. Neuroscience. 1977; 2:1–18. [PubMed: 72363]

Cottrell GA, Abernathy KB, Barrand MA. Large amine-containing neurons in the central ganglia of *Lymnaea stagnalis*. Neuroscience. 1979; 4:685–689. [PubMed: 450258]

Croll RP. Distribution of monoamines within the central nervous system of the pulmonate snail *Achatina fulica*. Brain Res. 1988; 460:29–49. [PubMed: 3064870]

Croll RP. Catecholamine-containing cells in the central nervous system and periphery of *Aplysia californica*. J Comp Neurol. 2001; 441:91–105. [PubMed: 11745637]

Croll RP, Chiasson BJ. Distribution of catecholamines and of immunoreactivity to substances like vertebrate enzymes for the synthesis of catecholamines within the central nervous system of the snail, *Lymnaea stagnalis*. Brain Res. 1990; 525:101–114. [PubMed: 1978788]

Croll RP, Voronezhskaya EE, Hiripi L, Elekes K. Development of catecholaminergic neurons in the pond snail *Lymnaea stagnalis*. II. Postembryonic development of central and peripheral cells. J Comp Neurol. 1999; 404:297–309. [PubMed: 9952349]

Croll RP, Boudko DY, Pires A, Hadfield MG. Transmitter contents of cells and fibres in the cephalic sensory organs of the gastropod mollusc *Phestilla sibogae*. Cell Tissue Res. 2003; 314:437–448. [PubMed: 14598161]

Croll RP, Chiasson BJ. Distribution of catecholamines and of immunoreactivity to substances like vertebrate enzymes for the synthesis of catecholamines within the central nervous system of the snail, *Lymnaea stagnalis*. Brain Res. 1990; 525:101–114. [PubMed: 1978788]

Cropper EC, Evans CG, Hurwitz I, Jing J, Proekt A, Romero A, Rosen SC. Feeding neural networks in the mollusk *Aplysia*. Neurosignals. 2004; 13:70–86. [PubMed: 15004426]

Dahl E, Falck B, von Mecklenburg C, Myhrberg H, Rosengran E. Neuronal localization of dopamine and 5-hydroxytryptamine in some Mollusca. Zeitschrift für Zellforschung. 1966; 71:489–498.

de Jong-Brink M. How schistosomes profit from the stress responses they elicit in their hosts. Adv Parasitol. 1995; 35:177–256. [PubMed: 7709853]

de Jong-Brink M, Bergamin-Sassen M, Solis Soto M. Multiple strategies of schistosomes to meet their requirements in the intermediate snail host. Parasitology. 2001; 123(Suppl):S129–141. [PubMed: 11769278]

Delgado, N.; Vallejo, DI.; Miller, MW. Neuroscience Meeting Planner. San Diego, CA: Society for Neuroscience; 2010. Localization of biogenic amines in the pond snail *Biomphalaria glabrata*. Program No.783.1.2010, Online

Delgado N, Vallejo D, Miller MW. Localization of serotonin in the nervous system of *Biomphalaria glabrata*, an intermediate host for schistosomiasis. J Comp Neurol. 2012; 520:3236–3255. [PubMed: 22434538]

Díaz-Ríos M, Miller MW. Rapid dopaminergic signaling by interneurons that contain markers for catecholamines and GABA in the feeding circuitry of *Aplysia*. J Neurophysiol. 2005; 93:2142–2156. [PubMed: 15537820]

Due MR, Jing J, Weiss KR. Dopaminergic contribution to modulatory functions of a dual-transmitter interneuron in *Aplysia*. Neurosci Lett. 2004; 358:53–57. [PubMed: 15016433]

Elekes K, Kemenes G, Hiripi L, Geffard M, Benjamin PR. Dopamine-immunoreactive neurones in the central nervous system of the pond snail *Lymnaea stagnalis*. J Comp Neurol. 1991; 307:214–224. [PubMed: 1713231]

Emery DG. Fine structure of olfactory epithelia of gastropod molluscs. Microsc Res Tech. 1992; 22:207–224. [PubMed: 1504352]

Etges FJ, Decker CL. Chemosensitivity of the miracidium of *Schistosoma mansoni* to *Australorbis glabratus* and other snails. J Parasitol. 1963; 49:114–116.

Etges FJ, Carter OS, Webbe G. Behavioral and developmental physiology of schistosome larvae as related to their molluscan hosts. Ann NY Acad Sci. 1975; 266:480–496. [PubMed: 801112]

Faller S, Stauback S, Klussman-Kolb A. Comparative immunohistochemistry of the cephalic sensory organs in Opisthobranchia (Mollusca, Gastropoda). Zoomorphology. 2008; 127:227–239.

Furness JB, Costa M, Wilson AJ. Water-soluble fluorophores, produced by reaction with aldehyde solutions, for the histochemical localization of catechol- and indolethylamines. Histochemistry. 1977; 52:159–170. [PubMed: 406252]

Geraerts WPM, Joose J. Control of vittelogenesis and of growth of female accessory sex organs by the Dorsal Body Hormone (DBH) in the hermaphrodite freshwater snail *Lymnaea stagnalis*. Gen Comp Endocrinol. 1975; 27:450–464. [PubMed: 1218695]

Geraerts WPM, Algera LH. The stimulating effects of the dorsal-body hormone on cell differentiation in the female accessory sex organs of the hermaphrodite freshwater snail, *Lymnaea stagnalis*. Gen Comp Endocrin. 1976; 29:109–118.

Hamdan FF, Ribeiro P. Cloning and characterization of a novel form of tyrosine hydroxylase from the human parasite, *Schistosoma mansoni*. J Neurochem. 1998; 71:1369–1380. [PubMed: 9751167]

Harris SJ, Cottrell GA. Properties of an identified dopamine-containing neuron in culture from the snail *Helisoma*. Exp Physiol. 1995; 80:37–51. [PubMed: 7734137]

Hauser M, Koopowitz H. Age-dependent changes in fluorescent neurons in the brain of *Notoplana acticola*, a polyclad flatworm. J Exp Zool. 1987; 241:217–225. [PubMed: 3559506]

Hernádi L, Elekes K, S-Rózsa K. Distribution of serotonin-containing neurons in the central nervous system of the snail *Helix pomatia*. Cell and Tissue Res. 1989; 257:313–323.

Hernadi L, Juhos S, Elekes K. Distribution of tyrosine-hydroxylase-immunoreactive and dopamine-immunoreactive neuronesin the central nervous system of the snail *Helix pomatia*. Cell Tissue Res. 1993; 274:503–513.

Hernádi L, Elekes K. Topographic organization of serotonergic and dopaminergic neurons in the cerebral ganglia and their peripheral projection patterns in the head areas of the snail *Helix aspersa*. J Comp Neurol. 1999; 411:274–287. [PubMed: 10404253]

Hotez, PJ. Forgotten people, forgotten diseases: the neglected tropical diseases and their impact on global health and development. Washington, DC: American Society of Microbiology; 2008.

Joosse J. Dorsal bodies and dorsal neurosecretory cells of the cerebral ganglia of *Lymnaea stagnalis*. Arch Néerl Zool. 1964; 16:1–103.

Kabotyanski EA, Baxter DA, Byrne JH. Identification and characterization of catecholaminergic neuron B65, which initiates and modifies patterned activity in the buccal ganglia of *Aplysia*. J Neurophysiol. 1998; 79:606–621.

Kabotyanski EA, Baxter DA, Cushman SJ, Byrne JH. Modulation of fictive feeding by dopamine and serotonin in *Aplysia*. J Neurophysiol. 2000; 83:374–392. [PubMed: 10634881]

Katz PS. Intrinsic and extrinsic neuromodulation of motor circuits. Curr Opin Neurobiol. 1995; 5:99–808.

Katz, PS.; Edwards, DH. Metamodulation:the control and modulation of neuromodulation. In: Katz, PS., editor. Beyond Neurotransmission. New York: Oxford University Press; 1999. p. 349-381.

Katz PS, Frost WN. Intrinsic neuromodulation: altering neuronal circuits from within. Trends Neurosci. 1996; 19:54–61. [PubMed: 8820868]

Kemenes K, Elekes K, Hiripi L, Benjamin PR. A comparison of four techniques for mapping the distribution of serotonin and serotonin-containing neurons in fixed and living ganglia of the snail, *Lymnaea*. J Neurocytology. 1989; 18:193–208.

Kiehn L, Saleuddin S, Lange A. Dopaminergic neurons in the brain and dopaminergic innervation of the albumen gland in mated and virgin *Helisoma duryi* (Mollusca: Pulmonata). BMC Physiology. 2001; 1:9. [PubMed: 11513757]

King CH. Parasites and poverty: the case of schistosomiasis. Acta Trop. 2010; 113:95–104. [PubMed: 19962954]

Koene JM. Neuro-endocrine control of reproduction in hermaphroditic freshwater snails: mechanisms and evolution. Front in Behav Neurosci. 201010.3389/fnbeh.2010.00167

Kupfermann I, Weiss KR. Motor program selection in simple model systems. Curr Opin Neurobiol. 2001; 11:673–677. [PubMed: 11741016]

Kyriakides MA, McCrohan CR. Effect of putative neuromodulators on rhythmic buccal motor output in *Lymnaea stagnalis*. J Neurobiol. 1989; 20:635–650. [PubMed: 2794997]

Larsen MB, Fontana ACK, Magalhães, Rodrigues V, Mortensen OV. A catecholamine transporter from the human parasite *Schistosoma mansoni* with low affinity for psychostimulants. Mol Biochem Parasitol. 2011; 177:35–41. [PubMed: 21251927]

Lefèvre T, Adamo SA, Biron DG, Missé D, Hughes D, Thomas D. Invasion of the body snatchers: the diversity and evolution of manipulative strategies in host-parasite interactions. Adv Parasitol. 2009

Lever J, de Vries CM, Jager JC. On the anatomy of the central nervous system and the location of neurosecretory cells in *Australorbis glabratus*. Malacologia. 1965; 2:219–230.

Loker ES, Cimino DF, Hertel LA. Excretory-secretory products of *Echinostoma paraensei* sporocysts mediate interference with *Biomphalaria* hemocyte functions. J Parasitol. 1992; 78:104–115. [PubMed: 1738052]

Magoski NS, Bauce LG, Syed NI, Bulloch AGM. Dopaminergic transmission between identified neurons from the mollusk, *Lymnaea stagnalis*. J Neurophysiol. 1995; 74:1287–1300. [PubMed: 7500151]

Maldonado, JF. Schistosomiasis in America. Editorial Cientifico-Medica; Barcelona: 1967.

Manger P, Li J, Christensen BM, Yoshino TP. Biogenic monoamines in the freshwater snail, *Biomphalaria glabrata*: Influence of infection by the human blood fluke, *Schistosoma mansoni*. Comp Biochem Physiol. 1996; 114A:227–234.

Marsden C, Kerkut GA. The occurrence of monoamines in *Planorbis corneus*: a fluorescence microscopic and microspectrometric study. Comp Gen Pharmacol. 1970; 1:101–116. [PubMed: 5527538]

McCaman MW, Ono JK, McCaman RE. Dopamine measurements in molluscan ganglia and neurons using a new, sensitive assay. J Neurochem. 1979; 32:1111–1113. [PubMed: 430045]

Meuleman EA. Host-parasite interrelationships between the freshwater pulmonate *Biomphalaria pfeifferi* and the trematode *Schistosoma mansoni*. Neth J Zool. 1972; 22:355–427.

Moroz LL, Winlow W. Respiratory behavior in *Lymnaea stagnalis*: pharmacological and cellular analyses. Acta Biol Hung. 1992; 3:88.

Murphy AD. The neuronal basis of feeding in the snail, *Helisoma*, with comparisons to selected gastropods. Prog Neurobiol. 2001:383–408. [PubMed: 11163684]

Nakamura H, Kojima S, Kobayashi S, Ito I, Fujito Y, Suzuki H, Ito E. Physiological characterization of lip and tentaclenerves in *Lymnaea stagnalis*. Neurosci Res. 1999a; 33:291–298. [PubMed: 10401982]

Nakamura H, Ito I, Kojima S, Fujito Y, Suzuki H, Ito E. Histological characterization of lip and tentacle nerves in *Lymnaea stagnalis*. Neurosci Res. 1999b; 33:127–136. [PubMed: 10211778]

Nargeot R, Baxter DA, Patterson GW, Byrne JH. Dopaminergic synapses mediate neuronal changes in an analogue of operant conditioning. J Neurophysiol. 1999; 81:1983–1987. [PubMed: 10200235]

Narusuye K, Nagahama T. Cerebral CBm1 neuron contributes to synaptic modulation appearing during rejection of seaweed in *Aplysia kurudai*. J Neurophysiol. 2002; 88:2778–2795. [PubMed: 12424312]

Osborne NN. Biochemical aspects of dopamine (3,4-dihydroxyphenethylamine) in an invertebrate nervous system: uptake, metabolism, and analysis of receptors. Biochem Soc Trans. 1977; 5:858–863. [PubMed: 21112]

Osborne NN, Cottrell GA. Distribution of biogenic amines in the slug, *Limax maximus*. Z Zeliforsch. 1971; 112:15–30.

Osborne NN, Guthrie PB, Neuhoff V. Tyrosine hydroxylase in snail (*Helix pomatia*) nervous tissue. Biochem Pharmacol. 1976; 25:925–931. [PubMed: 5096]

Osborne NN, Priggemeier E, Neuhoff V. Dopamine metabolism in characterized neurones of *Planorbis corneus*. Brain Res. 1975; 90:261–271. [PubMed: 1139307]

Pan C-T. Studies on the host-parasite relationship between *Schistosoma mansoni* and the snail *Australorbis glabratus*. Am J Trop Med and Hygiene. 1965; 14:931–976.

Pentreath VW, Berry MS, Cottrell GA. Anatomy of the giant dopamine-containing neurone in the left pedal ganglion of *Planorbis corneus*. Cell Tissue Res. 1974; 151:369–384. [PubMed: 4426076]

Quinlan EM, Arnett BC, Murphy AD. Feeding stimulants activate an identified dopaminergic interneuron that induces the feeding motor program in *Helisoma*. J Neurophysiol. 1997; 78:812–824. [PubMed: 9307115]

Rollinson, D.; Chappell, LH. Flukes and snails revisited. Cambridge University Press; London: 2002.

Rosen SC, Teyke T, Miller MW, Weiss KR, Kupfermann I. Identification and characterization of cerebral-to-buccal interneurons implicated in the control of motor programs associated with feeding in *Aplysia*. J Neurosci. 1991; 11:3630–3655. [PubMed: 1941100]

Roubos EW, Van der Ven AMH. Morphology of neuroscecretory cells in basommatophoran snails homologous with eff-laying and growth-hormone producing cells of *Lymnaea stagnalis*. Gen Comp Endocrinol. 1987; 67:7–23. [PubMed: 3623071]

Sakharov DA, Voronezhskaya EE, Nezlin L, Baker MW, Elekes K, Croll RP. Tyrosine hydroxylase-negative, dopaminergic neurons are targets for transmitter-depleting action of haloperidol in the snail brain. Cell Mol Neurobiol. 1996; 16:451–61. [PubMed: 8879748]

Saleuddin ASM, Kukai ST, Almeida K, Hatiras G. Membrane transduction pathway in the neuronal control of protein secretion by the albumen gland in *Helisoma* (Mollusca). Acta Biol Hung. 2000; 51:243–253. [PubMed: 11034149]

Salimova NB, Sakharov DA, Milosevic I, Rakic L. Catecholamine-containing neurons in the peripheral nervoussystem of *Aplysia*. Acta Biol Hung. 1987; 38:203–212. [PubMed: 3454082]

Santhanagopalan V, Yoshino TP. Monoamines and their metabolites in the freshwater snail *Biomphalaria glabrata*. Comp Biochem Physiol A Mol Integr Physiol. 2000; 125:469–478. [PubMed: 10840222]

Slade CT, Mills J, Winlow W. The neuronal organization of the paired pedal ganglia of *Lymnaea stagnalis* (L.). Comp Biochem Physiol A. 1981; 69:789–803.

Sweeney D. Dopamine: its occurrence in molluscan ganglia. Science. 1963; 139:1051. [PubMed: 13979659]

Syed NI, Winlow W. Morphology and electrophysiology of neurons innervating the ciliated locomotor epithelium in *Lymnaea stagnalis* (L.). Comp Biochem Physiol [A}. 1989; 93:633–644.

Syed NI, Winlow W. Respiratory behavior in the pond snail *Lymnaea stagnalis*. II. Neural elements in the central pattern generator (CPG). J Comp Physiol [A]. 1991; 169:557–568.

Syed NI, Bulloch AGM, Lukowiak KL. *In vitro* reconstruction of the respiratory central pattern generator (CPG) of the mollusk *Lymnaea*. Science. 1990; 250:282–285. [PubMed: 2218532]

Syed NI, Ridgway RL, Lukowiak K, Bulloch AGM. Transplantation and functional integration of an identified respiratory interneuron in *Lymnaea stagnalis*. Neuron. 1992; 8:767–774. [PubMed: 1314624]

Syed NI, Roger I, Ridgway RL, Bauce LG, Lukowiak K, Bulloch AGM. Identification, characterization, and *in vitro* reconstruction of an interneuronal network of the snail, *Helisoma trivolvis*. J exp Biol. 1993; 174:19–44. [PubMed: 8440965]

Taman A, Ribeiro P. Investigation of a dopamine receptor in *Schistosoma mansoni*: functional studies and immunolocalization. Mol Biochem Parasitol. 2009; 168:24–33. [PubMed: 19545592]

Taft AS, Norante FA, Yoshino TP. The identification of inhibitors of *Schistosoma mansoni* miracidial transformation by incorporating a medium-throughput small-molecule screen. Exp Parasitol. 2010; 125:84–94. [PubMed: 20060828]

Teyke T, Rosen SC, Weiss KR, Kupfermann I. Dopaminergic neuron B20 generates rhythmic neuronal activity in the feeding motor circuitry of *Aplysia*. Brain Res. 1993; 630:226–237. [PubMed: 8118689]

Toledo, R.; Fried, B., editors. Biomphalaria snails and larval trematodes. NY: Springer Press; 2010.

Trimble DL, Barker DL. Activation by dopamine of patterned motor output from the buccal ganglia of *Helisoma trivolvis*. J Neurobiol. 1984; 15:37–48. [PubMed: 6321653]

Trimble DL, Barker DL, Bullard BJ. Dopamine in a molluscan nervous system: synthesis and fluorescence histochemistry. J Neurobiol. 1984; 15:27–36. [PubMed: 6699633]

Vallejo, DI.; Delgado, N.; Blagburn, JM.; Miller, MW. Neuroscience Meeting Planner. Washington, DC: Society for Neuroscience; 2011. Tyrosine hydroxylase-like immunoreactive neurons in the central and peripheral nervous systems of *Biomphalaria glabrata*: Evidence for a role in chemoreception. Program No. 707.06.2011, Online

Wentzell MM, Martínez-Rubio C, Miller MW, Murphy AD. Comparative neurobiology of feeding in the opisthobranch sea slug, *Aplysia*, and the pulmonate snail, *Helisoma*: evolutionary considerations. Brain Behav Evol. 2009; 74:219–230. [PubMed: 20029185]

Werkman TR, De Vlieger TA, Stoof JC. Indications for a hormonal function of dopamine in the central nervous system of the snail *Lymnaea stagnalis*. Neurosci Letts. 1990; 108:167–172. [PubMed: 2304625]

Werkman TR, van Minnen J, Voorn P, Steinbusch HW, Westerink BH, De Vlieger TA, Stoof JC. Localization of dopamine and its relation to the growth hormone producing cells in the central nervous system of the snail *Lymnaea stagnalis*. Exp Brain Res. 1991; 85:1–9. [PubMed: 1715823]

Wieland SJ, Gelperin A. Dopamine elicits feeding motor program in *Limax maximus*. J Neurosci. 1983; 3:1735–1745. [PubMed: 6886743]

Wieland SJ, Jahn E, Gelperin A. Localization and synthesis of monoamines in regions of *Limax* CNS controlling feeding behavior. Comp Biochem Physiol C. 1987; 86:125–130. [PubMed: 2881707]

Williams CL, Gilbertson DE. Altered feeding responses as a cause for the altered heartbeat rate and locomotor activity of *Schistosoma mansoni*-infected *Biomphalaria glabrata*. J Parasitol. 1983; 69:671–676. [PubMed: 6631636]

Winlow W, Haydon PG, Benjamin PR. Multiple postsynaptic actions of the giant dopamine-containing neurone R.Pe.D.1 of *Lymnaea stagnalis*. J exp Biol. 1981; 94:137–148.

World Health Organization. WHO Media Centre. Schistosomiasis. Fact sheet N°115. Geneva: WHO; 2011. www.who.int/mediacentre/factsheets/fs115/en/index.html

Wright CA. Host-location by trematode miracidia. Am Trop Med Parasitol. 1958; 53:288–292.

Wright, CA. Flukes and Snails. New York: Hafner Press; 1973.

Wyeth RC, Croll RP. Peripheral sensory cells in the cephalic sensory organs of *Lymnaea stagnalis*. J Comp Neurol. 2011; 519:1894–1913. [PubMed: 21452209]

Xin Y, Weiss KR, Kupfermann I. Distribution in the central nervous system of *Aplysia* of afferent fibers arising from cell bodies located in the periphery. J Comp Neurol. 1995; 359:627–643. [PubMed: 7499552]

Yoshino TP, Lodes MJ, Rege AA, Chappell CL. Proteinase activity in miracidia, transformation excretory-secretory products, and primary sporocysts of *Schistosoma mansoni*. J Parasitol. 1993; 79:23–31. [PubMed: 8437057]

Yoshino TP, Boyle JP, Humphries JE. Receptor-ligand interactions and cellular signaling at the host-parasite interface. Parasitology. 2001; 123:S143–S157. [PubMed: 11769279]

Zahoor Z, Davies AJ, Kirk RS, Rollinson D, Walker AJ. Nitric oxide production by *Biomphalaria* haemocytes: effects of *Schistsoma mansoni* ESPs and regulation through the extracellular signal-regulated kinase pathway. Parasites & Vectors. 2009; 2:18. [PubMed: 19386102]

Zaitseva OV. Structural organization of the sensory systems of the snail. Neurosci Behav Physiol. 1994; 24:47–57. [PubMed: 8208381]

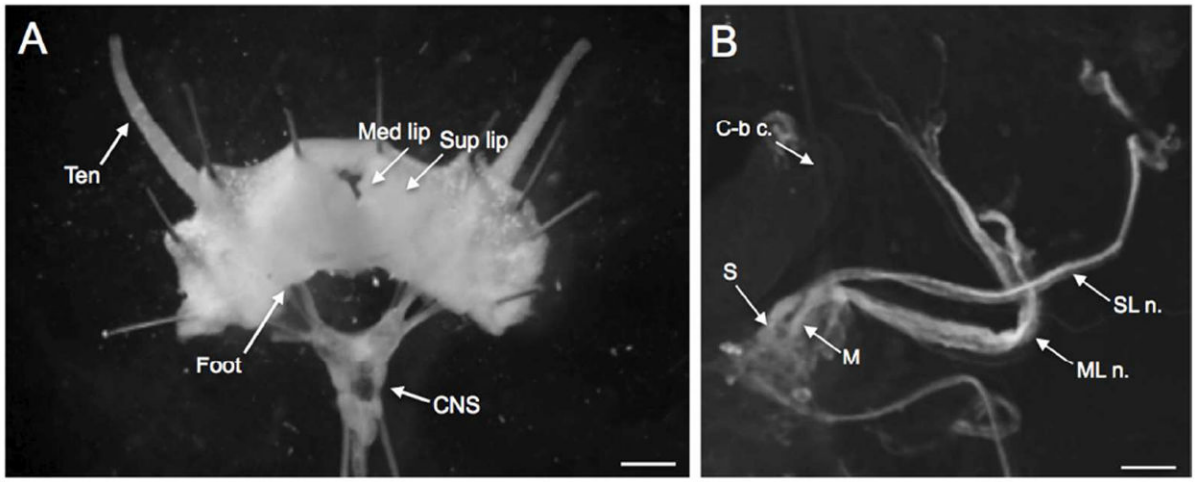


**Figure 1.**

The *Biomphalaria* head-brain preparation developed to examine innervation of cephalic structures. **A:** Following a dorsal midline incision, the cephalic structures were reflected laterally exposing the innervation of the tentacle (*Ten*), superior lip (*Sup lip*), and medial lip (*Med lip*). The anterior portion of the *foot* was also retained in this preparation. The digestive system, reproductive structures, and the buccal mass were removed to enable examination of the circumesophageal ring (*CNS*) and the nerves innervating the head. Scale bar= 0.5 mm. **B:** Right dorsolateral quadrant of the cerebral ganglion. The superior lip nerve (*SL n.*) originates from a more medial position than the medial lip nerve (*ML n.*) and the two nerves cross in the periphery. The cerebral-buccal connective (*C-b c.*) emerges from the ventral surface of the ganglion and is not in focus in this image. Scale bar = 100 μm.

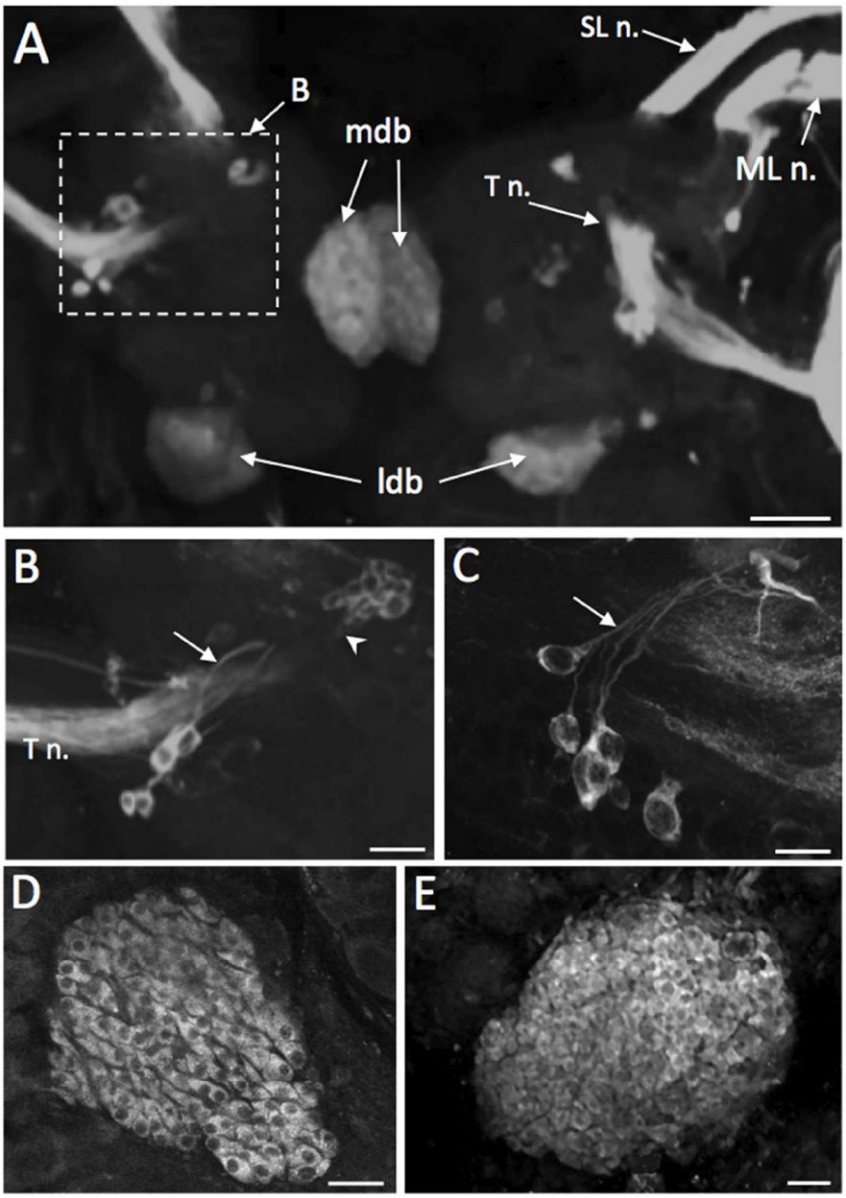


**Figure 2.**

TH-like immunoreactivity on the dorsal aspect of the cerebral ganglion. **A:** Dorsal surface of *Biomphalaria glabrata* cerebral ganglion. The superior lip nerve (*SL n.*), medial lip nerve (*ML n.*), and the tentacular nerve (*T n.*) are densely filled with immunoreactive fibers. Several neurons are located near the origin of origin of each *T n.* (*dashed box B*). Diffuse staining is present in the medial dorsal bodies (*mdb*) adjacent to the cerebral commissure and the lateral dorsal bodies (*ldb*) bordering the posterior margin of each hemiganglion. Scale bar = 100 μm. **B:** Region enclosed by *dashed box* in panel *A*; not from the same preparation. Neurons with prominent axons (*arrow*) near the origin of the tentacular nerve of *B. glabrata*. An aggregate of ten to twelve small (10-20 μm) THli neurons (*arrowhead*) is also observed anteromedial to the *T n.* origin. Scale bar = 50 μm. **C:** Neurons with prominent axons (*arrow*) near the origin of the T n. in *B. alexandrina*. Scale bar = 50 μm. **D:**

Densely packed elongated profiles in the dorsal body of *B. alexandrina*. A prominent unstained nucleus is present in each cell. Scale bar = 20 μm. **E:** The lateral dorsal body cortex of *B. glabrata* is filled with small perikarya of varied sizes (5-10 μm) and shapes. Scale bar = 30 μm.

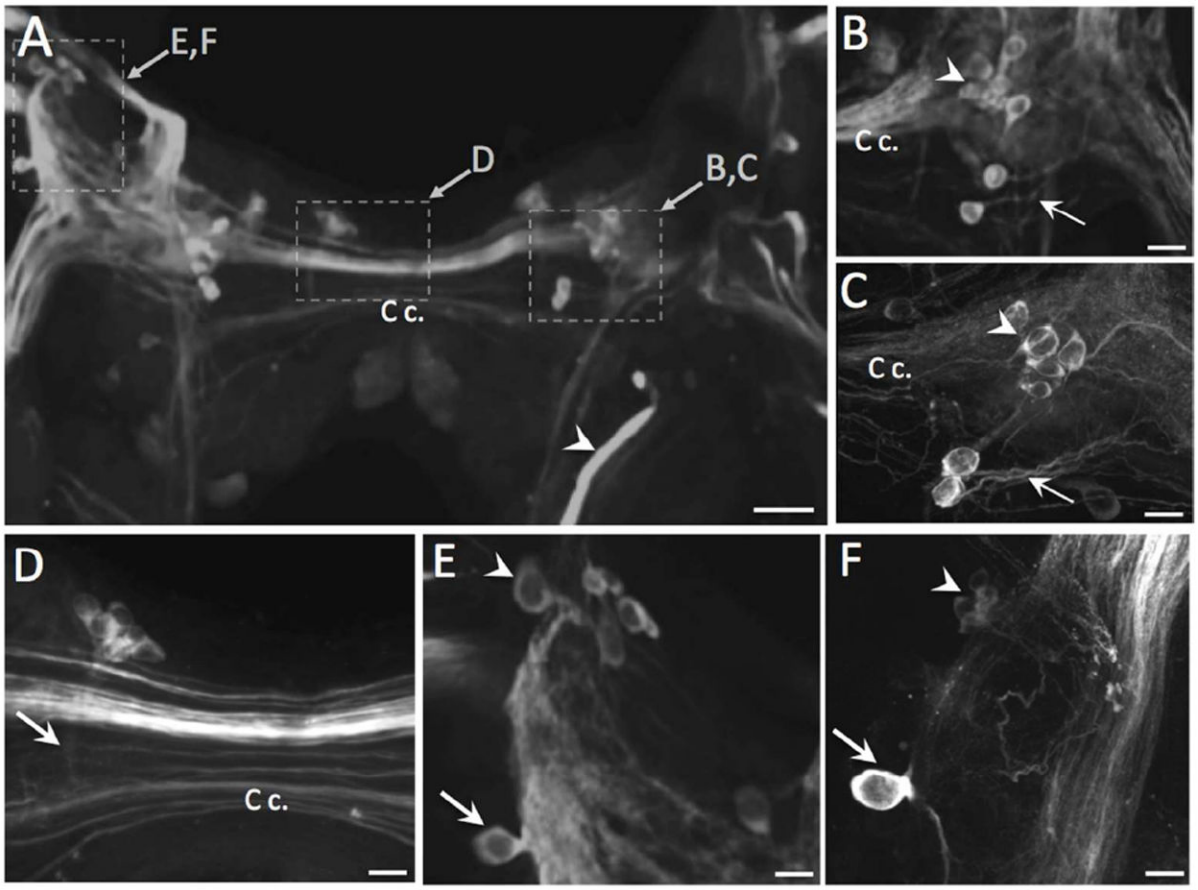


**Figure 3.**

TH-like immunoreactivity on the ventral surface of the cerebral ganglion. **A:** A group of superficial neurons (*dashed box B, C*) is located near the confluence of intensely stained fiber tracts converging from the major cerebral nerves and the cerebral commissure (*C c.*). *B. glabrata* shown. Additional immunoreactive cell groups are present near the cerebral commissure (*dashed box D*) and at the anterolateral margin of ganglion near the origin of the medial lip nerve (*dashed box E, F*). Scale bar = 50 μm. **B**: Neurons near the convergence of the cerebral nerves on the ventral surface of the left cerebral hemiganglion (*B. glabrata*, not the same preparation as **A**). The axons of the two most intensely stained cells were oriented in the lateral direction, away from the *C c.* (*arrow*). Scale bar = 20 μm. **C:** Neurons near the convergence of the cerebral nerves and the cerebral commissure of *B. alexandrina*. The axons of the two most intensely stained cells were oriented in the lateral direction (*arrow*). Scale bar = 20 μm. **D:** Cerebral commissure of *B. glabrata* (same preparation as *A*). A cluster of small neurons in the anteromedial region of the right hemiganglion gives rise to a thin fascicle of fibers projecting in the posterior direction (*arrow*). Scale bar = 20 μm. **E:** THli neurons in the anterolateral lateral region of the *B. glabrata* cerebral ganglion (same preparation as *A*). A single neuron (*arrow*) is located lateral to the ML n. tract and a group of cells is positioned near the origin of the nerve (*arrowhead*). Scale bar = 20 μm. **F:** Anterolateral region of the ventral CG of *B. alexandrina*. The solitary neuron adjacent to the ML n. (*arrow*) projected one fiber toward the periphery and another centrally. As in *B.*

*glabrata*, a cluster of smaller neurons was present near the base of the ML n. (*arrowhead*). Scale bar = 20 μm.

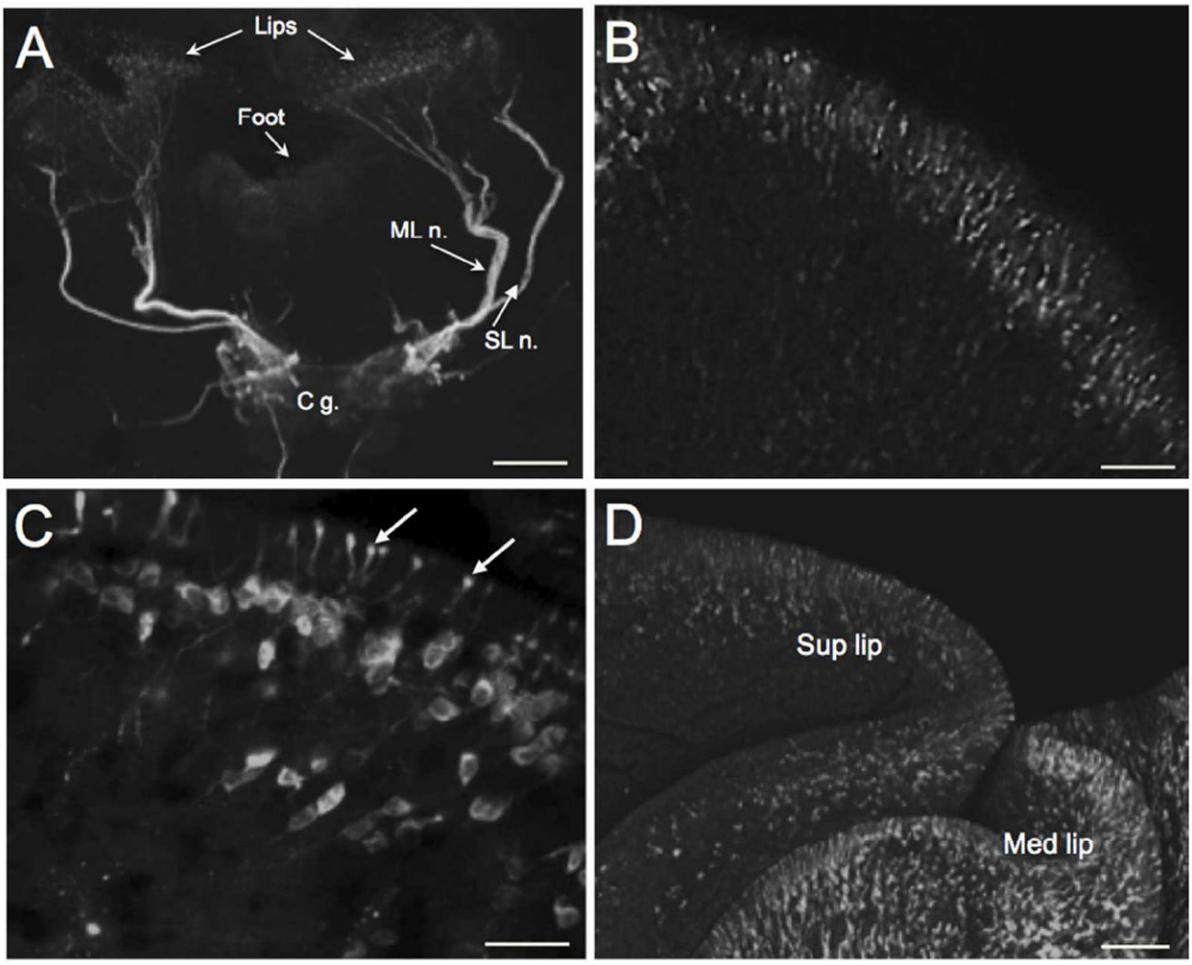


**Figure 4.**

THli cephalic peripheral neurons. **A:** Low magnification image of a *B. glabrata* head-brain preparation. The intensely stained medial lip nerve (*ML n.)* and the superior lip nerve (*SL n.*) originate from the cerebral ganglion (*C g.*). Both nerves branch in the periphery to innervate the lip epithelium. Scale bar = 200 μm. **B:** A layer of bipolar THli neurons lines the lip epithelium of *B. glabrata*. *Scale bar* = 50 μm. **C:** Projections from the peripheral THli neurons penetrate the mantle integument of *B. alexandrina* and end in bulbous enlargements at the surface of the epithelium. Scale bar = 50 μm. **D:** Image of external surface of the superior lip (*Sup lip*) and inferior lip (*Inf lip*) confirms penetration of the distal processes of the THli neurons. Scale bar = 100 μm.

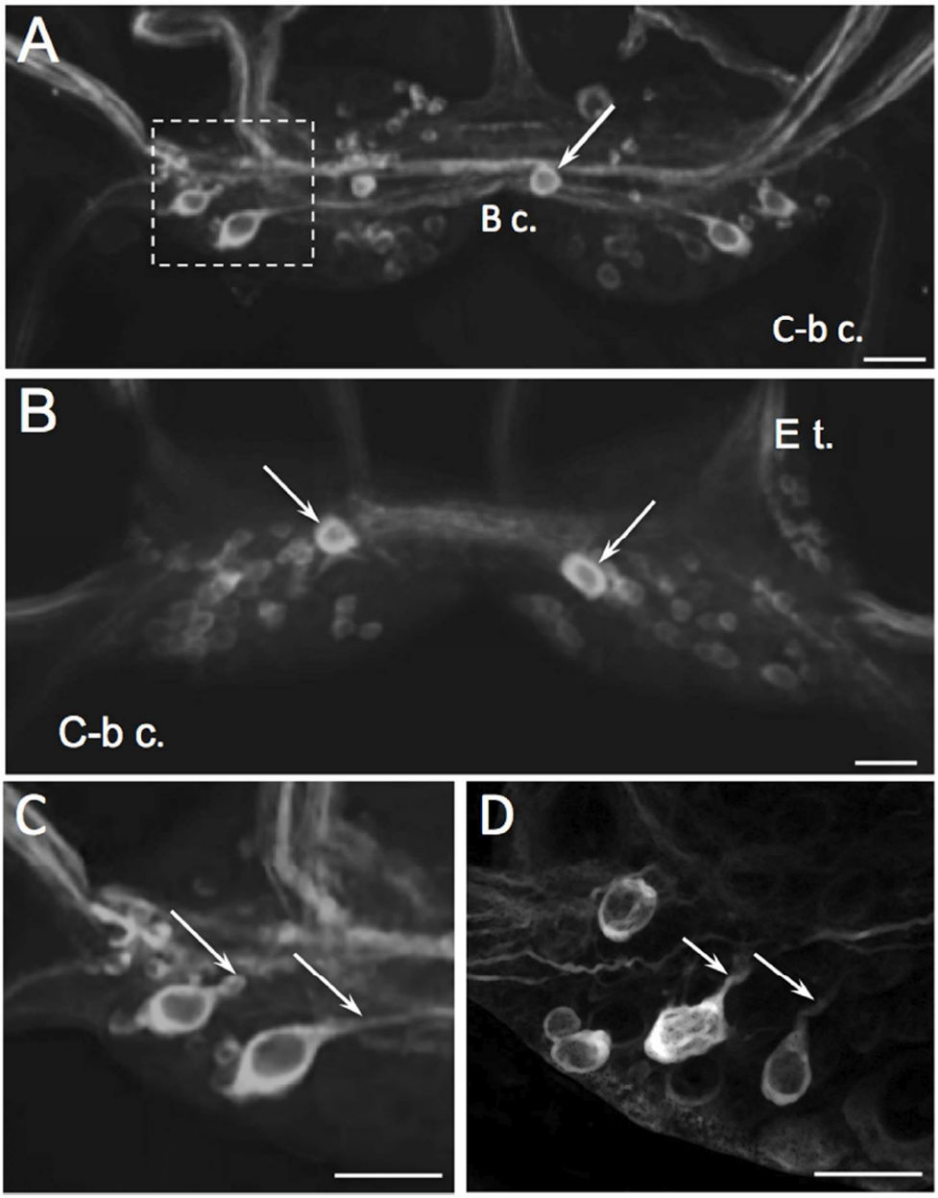


**Figure 5.**

TH-like immunoreactivity in the buccal ganglion. **A:** Asymmetric distribution of immunoreactive cell bodies on the caudal surface of the buccal ganglion of *B. glabrata*. Two lateral THli neurons are present in each buccal hemiganglion and an unpaired neuron (*arrow*) is located in the right buccal hemiganglion near the buccal commissure. Additional clusters of small (5 – 10 μm) weakly stained neurons are present in the ventromedial and dorsomedial region of each hemiganglion. Prominent THli fibers course through the buccal commissure (*B c.*) and in the buccal nerves. Two to three fibers were observed in each cerebral-buccal connective (*C-b c.*). Scale bar = 50 μm. **B:** Rostral surface of *B. glabrata* buccal ganglion. A single strongly immunoreactive cell (*arrows*) is located in each hemiganglion near the buccal commissure. Smaller cells with weaker staining are distributed through the medial regions of both hemiganglia. Scale bar = 50 μm. **C:** Higher

magnification of the two lateral caudal THli neurons (left buccal ganglion of *B. glabrata*, dashed rectangle of panel *A*). Both neurons project fibers toward the central commissural bundle (*arrows*). Scale bar = 40 μm. **D:** Lateral region of left buccal ganglion of *B. alexandrina*; dorsal surface, approximately same area shown for *B. glabrata* in *C*. Lateral THli neurons give rise to processes projecting toward the central commissural bundle (*arrows*). Scale bar = 40 μm.

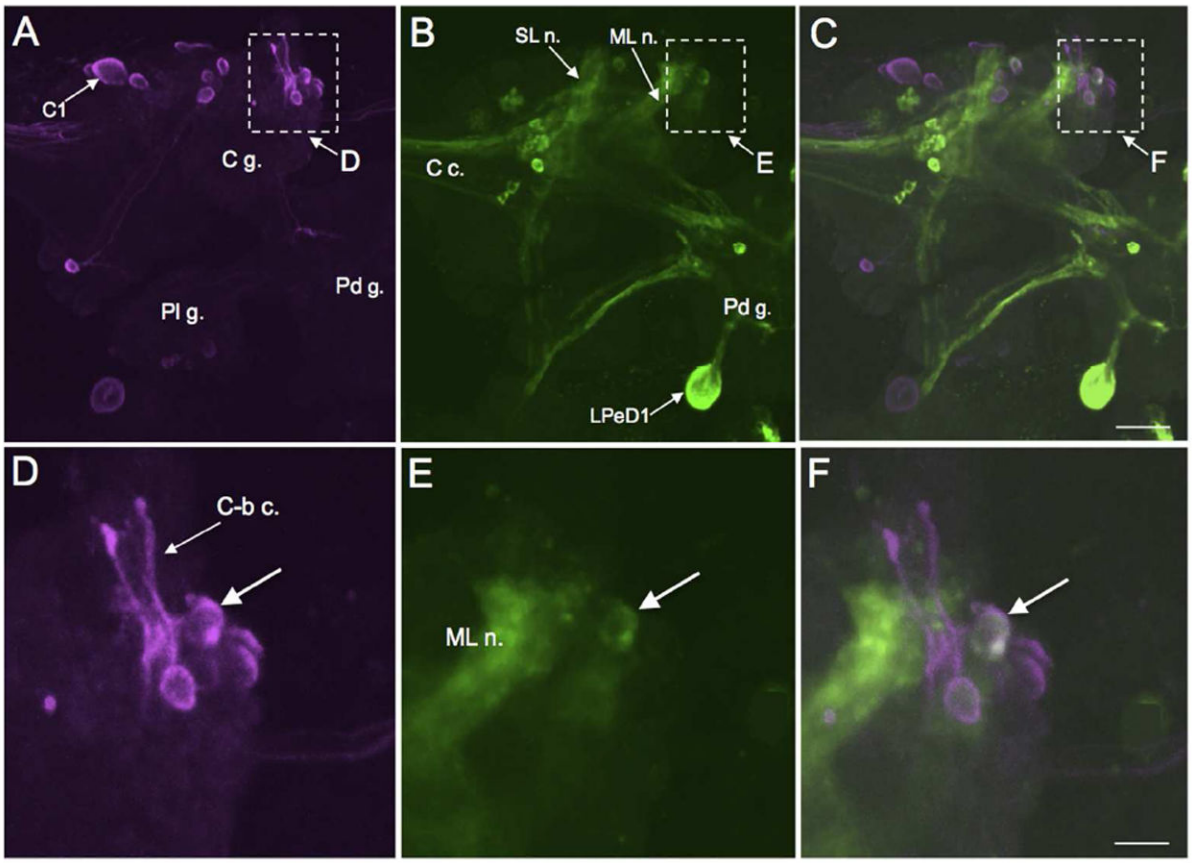


**Figure 6.**

Double-labeling of a THli cerebral-buccal interneuron. **A:** Biocytin backfill of the left cerebral-buccal connective of *B. glabrata* (ventral view). The majority of backfilled neurons (magenta), including the giant serotonergic *C1* cell, are located in the anterolateral region of the cerebral ganglion (*C g.*). *Dashed rectangle* indicates region shown in panel *D*. **B:** TH-like immunoreactivity (green); same field of view as *A*. The large *LPeD1* neuron appears on the dorsal surface of the pedal ganglion (*Pd g.*) which is retracted to facilitate visualization of the ventral aspect of the cerebral ganglion (see Methods). *Dashed rectangle* indicates region shown in panel *E*. **C:** Overlay of panels *A* and *B*. Double-labeled cell appears white. *Dashed rectangle* indicates region shown in panel *F*. Scale bar = 100 μm, applies to *A*-*C*. **D:** Higher magnification of region enclosed by dashed rectangle in **A**. Several backfilled neurons are located near the origin of the *C-b c*. **E:** Higher magnification of region enclosed by dashed rectangle in *B*. A small (15 – 20 μm) THli neuron (*arrow*) is located near the base of the C-b c. lateral to the medial lip nerve (*ML n.*). **F:** Overlay of panels *D* and *E*. Higher magnification of region enclosed by dashed rectangle in *C*. Double-labeling (white) is observed in the neuron at the base of the C-b c. lateral to the ML n. fiber tract (*arrow*). Scale bar = 30 μm, applies to D-F.

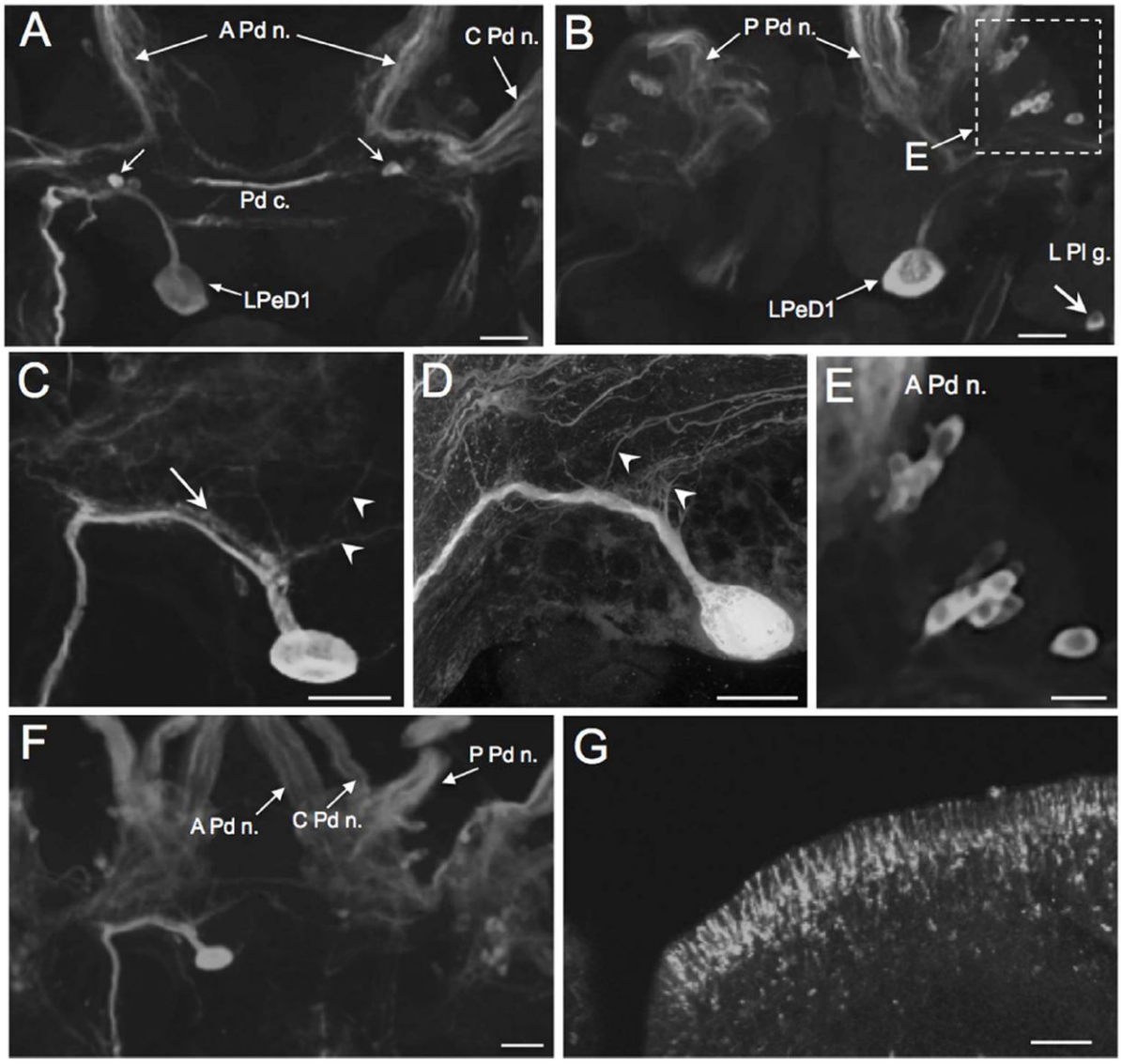


**Figure 7.**

TH-like immunoreactivity in the pedal ganglion. **A:** THli on the dorsal surface of the paired pedal ganglia (*Biomphalaria glabrata*). The prominent soma of the left pedal dorsal 1 (*LPeD1*) neuron is located medial to the statocyst on the posterior edge of the left pedal ganglion. Two small (10 – 15 μm) cells (*arrow*) are located in each pedal ganglion flanking the pedal commissure (*Pd c.*). The larger and more superficial neuron in each pair was more strongly stained and projected toward the pedal-pleural connective. Scale bar = 50 μm. **B:** THli on the ventral surface of the paired pedal ganglia; same preparation as *A*. Two clusters of neurons were positioned between the bases of the anterior pedal nerve and the central pedal nerve (*dashed rectangle*). Immunoreactive fibers were present in the posterior pedal nerve (*P Pd n.*) and in the pedal commissure (*Pd c.*). A single neuron was located on the posterior edge of the left pleural ganglion (*L Pl g.; arrow*). Scale bar = 50 μm. **C:** Higher magnification of the LPeD1 neuron of *B. glabrata*. Fine processes (*arrowheads*) project from the LPeD1 initial segment to the cerebral neuropil. Much of the major axon is flanked

by a fine network of immunoreactive fibres (*arrow*). Scale bar = 50 μm. **D:** LPeD1 neuron of *B. alexandrina*. Processes *(arrowheads*) project from the initial segment to the cerebral neuropil. Scale bar = 50 μm. **E:** Higher magnification of ventrolateral region of pedal ganglion enclosed by dashed rectangle in panel *A*. Two clusters of small neurons (10 – 15 μm) are oriented toward the medal Pd g. Scale bar = 30 μm. **F:** Cluster of small (10 – 15 μm; *arrow*) neurons in the central region of the left pedal ganglion of *B. alexandrina*. The initial segment of LPeD1 is visible in the lower part of this image (*arrowhead*). Scale bar = 30 μm. **G:** Immunoreactive neurons lining the anterior pedal integument. As with the neurons that innervate the lips (Fig. 4), distal processes from these cells penetrate the foot epithelium and end in bulbous swellings. Scale bar = 50 μm.

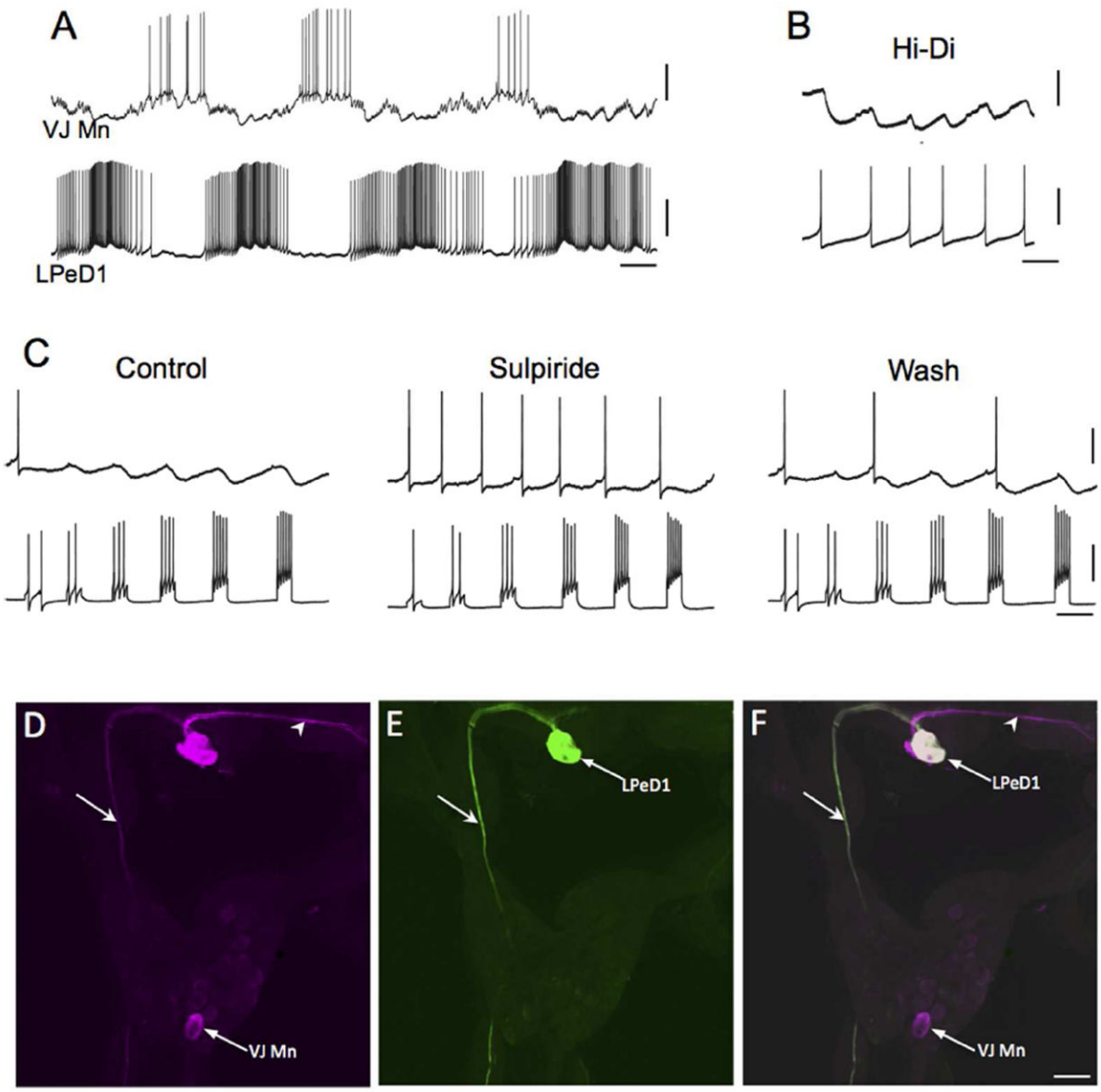


**Figure 8.**

Pharmacological support for the dopaminergic phenotype of labeled neurons. **A:** Intracellular recording from *LPeD1* (lower trace) of *B. glabrata*; isolated CNS in normal saline solution. The recording exhibits alternating phases of activity and quiescence. A putative cardio-respiratory motor neuron in the visceral ganglion (*VJ Mn*, upper trace) was observed to burst out of phase with LPeD1. Calibration bars: 5 s, 20 mV. **B:** Changing the bathing medium to a raised divalent saline solution (*Hi-Di*) eliminated polysynaptic signaling, enabling resolution of direct one-to-one inhibitory postsynaptic potential (IPSPs, upper record). Each IPSP occurred with a brief and constant latency following each LPeD1 impulse (lower record). Calibration bars = 1 s; 5 mV, upper record; 20 mV, lower record. **C:** Pharmacological evidence for direct dopaminergic signaling from LPeD1 to VJ Mn. *Control*: Depolarizing current pulses were passed into LPeD1 producing sequentially greater number of impulses (lower record). The IPSPs produced in the VJ Mn became progressively

larger as more impulses were stimulated. When the dopaminergic (D2) antagonist *sulpiride* was added to the solution (100 uM), the IPSPs were blocked. They returned following approximately 15 min Wash (*right panel*). Calibration bars = 0.5 s, 20 mV, 20 mV. **D-F:** Morphological confirmation of LPeD1 and VJ Mn identity. **D:** Neurobiotin was injected into *LPeD1*, a second neighboring cell in the pedal ganglion, and the *VJ Mn*. The three injected neurons were visualized with Avidin 546 (false color magenta). The axon of LPeD1 can be seen descending through the left pleural ganglion (*arrow*), while the neighboring cell projects to the contralateral pedal ganglion (*arrowhead*). **E:** When the preparation was processed for TH-like immunoreactivity and viewed with avidin 488 (green), only the LPeD1 neuron and its descending axon (arrow) were labeled. **F:** When the fill (D) and immunohistochemical (*E*) panels are overlaid, only the LPeD1 neuron and its descending axon (*arrow*) appear white (colocalization). The other injected cells, *VJ Mn* and the neighboring pedal neuron (*arrowhead*), appear magenta. Calibration bar = 50 μm, applies to D-F.

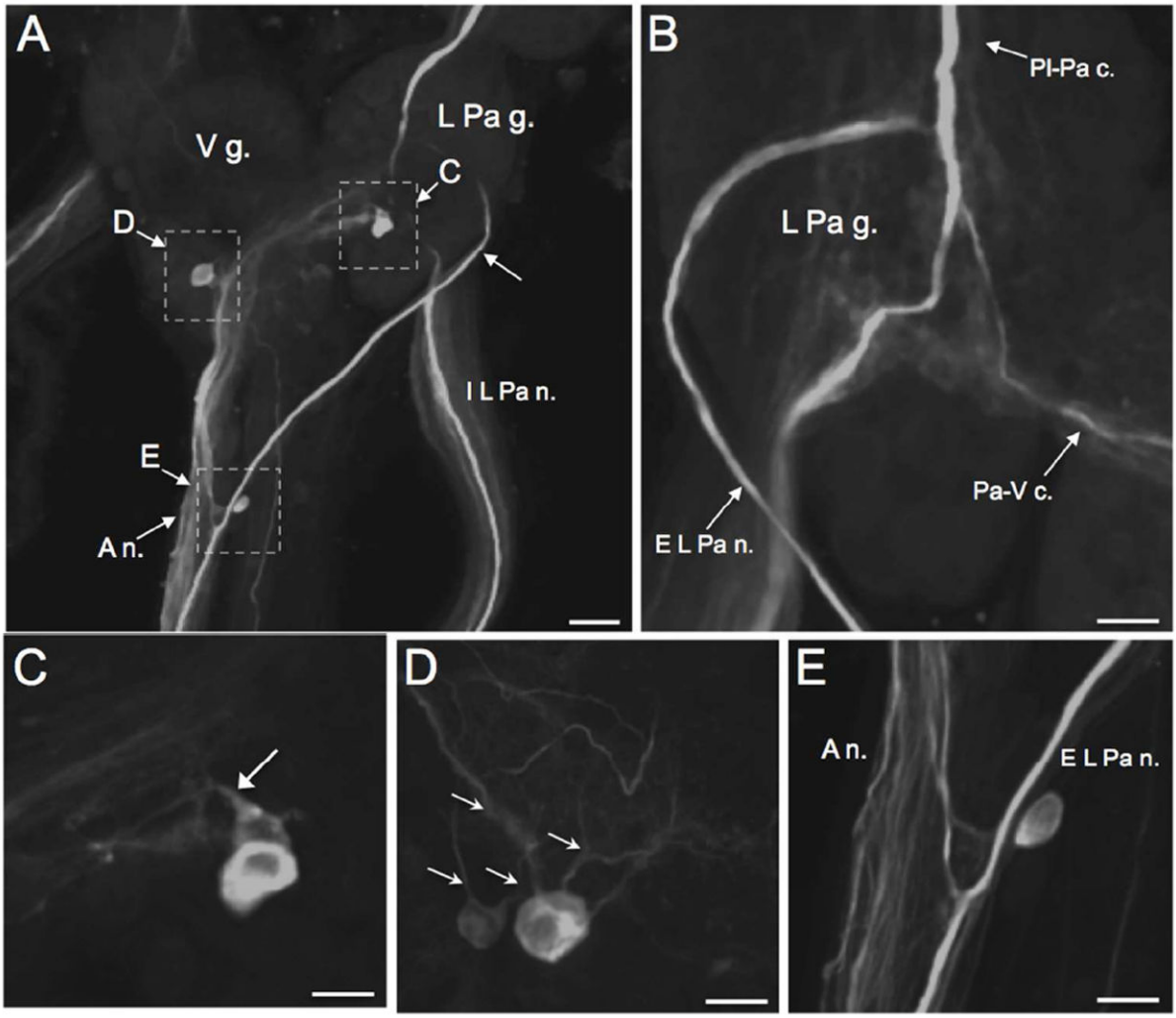


**Figure 9.**

TH-like immunoreactivity in the left parietal and visceral ganglia. **A:** Ventral surface of the left parietal ganglion (*L Pa g*.) and the visceral ganglion (*V g*.) of *B. glabrata*. The LPeD1 axon (*arrowhead*) descends to the central region of the L Pa g. where it gives rise to branches in the external left parietal nerve (*E L Pa n*.) and the internal left parietal nerve (*I L Pa n*.). Following fusion of the E L Pa n. with the anal nerve (*A n*.), the LPeD1 axon continued toward the periphery. *Dashed rectangles* indicate regions shown at higher magnification in panels *C, D* and *E*. Scale bar = 50 μm. **B:** Dorsal view of left parietal ganglion (*B. glabrata*) shows branch of LPeD1 projecting to the parietal-visceral connective (*Pa-V c*.). **C:** Two cell bodies in the central neuropil of the left parietal ganglion (*B. glabrata*). One of these cells is more superficial and larger (30 – 40 μm) than the other (20 – 30 μm), which is embedded in the central neuropil (*arrow*). Scale bar = 30 μm. **D:** Two immunoreactive cell bodies in the central neuropil of the visceral ganglion (*B. alexandrina*). Multiple fibers project from the somata of both cells (*arrows*). Scale bar = 30 μm. **E:** Anastomosis of the *E L Pa n*. and the *A n*. posterior to the visceral ganglion (*B. glabrata*). A single elongated neuron is embedded within the E L Pa n. Scale bar = 30 μm.

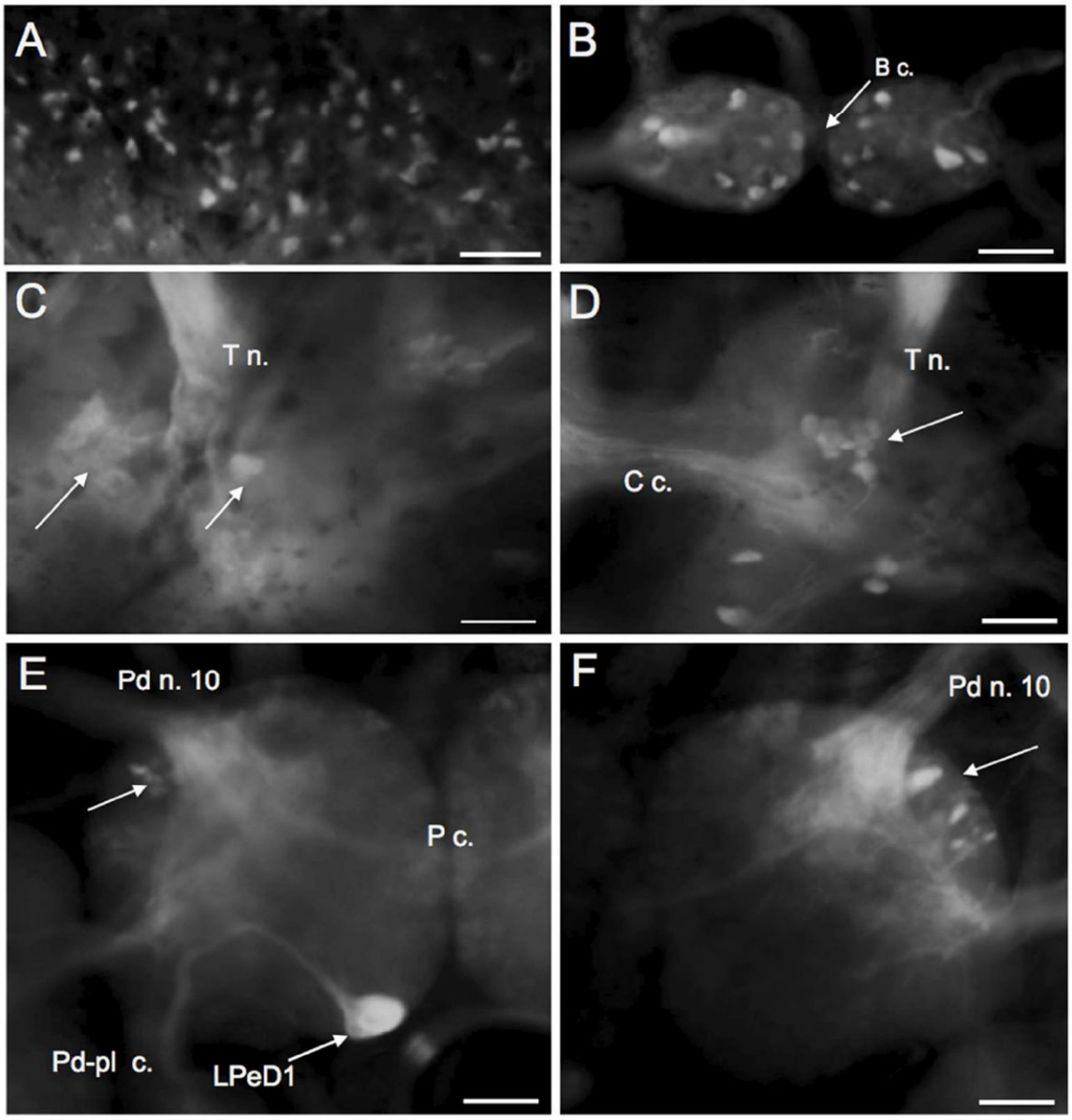


**Figure 10.**

FaGlu histofluorescence of catecholamines in the PNS and CNS of *Biomphalaria alexandrina*. **A:** Peripheral sensory cells in the lips. **B:** Two large intensely stained neurons (*arrows*) were located near the lateral edge of each buccal hemiganglion and groups of small neurons flanked the buccal commissure (*B c.*). **C:** Dorsal surface of the left cerebral ganglion. Intensely stained neurons were positioned near the origin of the tentacular nerve (T n.). **D:** Cluster of neurons on the mediodorsal surface of the right cerebral ganglion. **E:** The large LPeD1 neuron viewed from the dorsal surface of the left pedal ganglion with its large axon turning toward the pedal-pleural connective (*Pd-Pl c.*). A cluster of neurons (*arrow*) is located near the origin of pedal nerve 10 (*Pd n. 10*). **F:** Labeled neurons (*arrow*) were located near the origin of pedal nerve 10 on the dorsal surface of the right pedal ganglion. Scale bars = 50 μm, all panels.

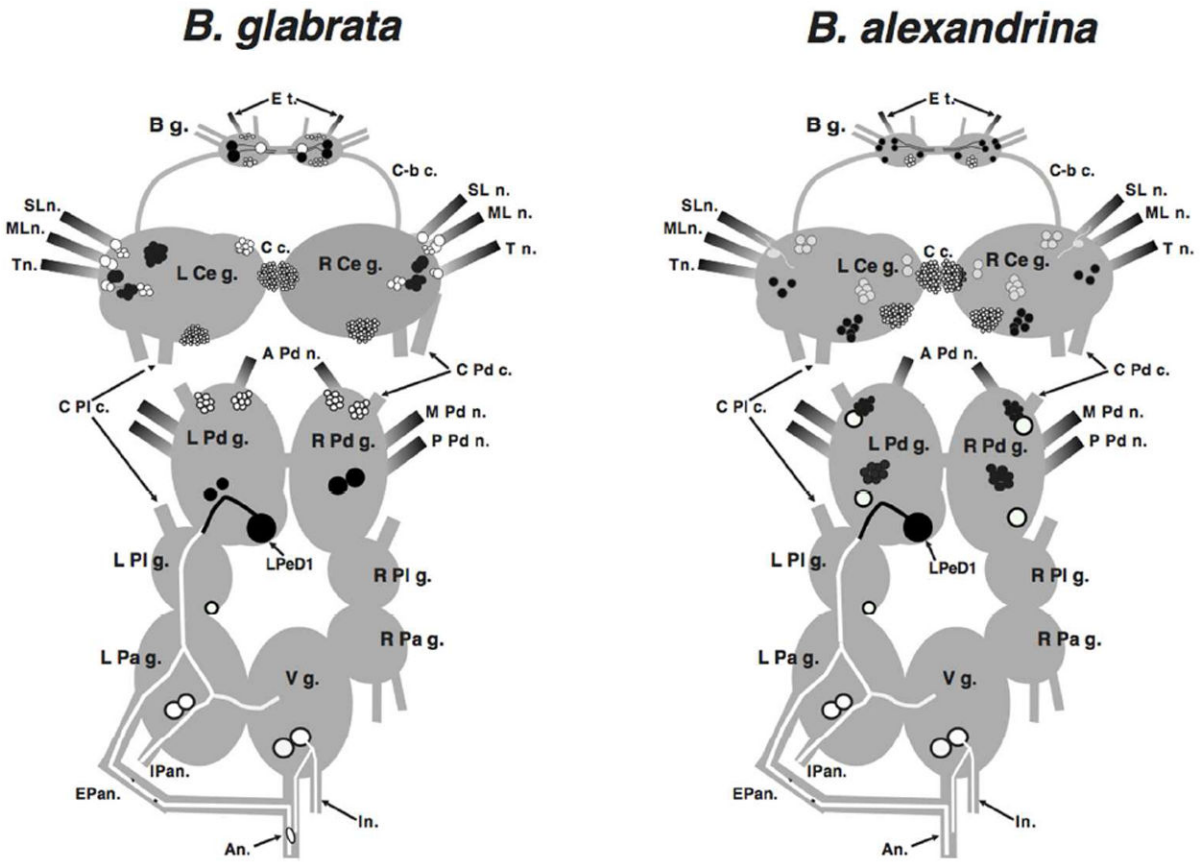


**Figure 11.**

Schematic representation of TH-like immunoreactivity in the central nervous system of *Biomphalaria glabrata* and *Biomphalaria alexandrina*. Dorsal view; the cerebral-pleural and cerebral-pedal connectives have been severed and the cerebral ganglia have been shifted upward to expose the pedal ganglia. Black profiles represent THli cell bodies on the dorsal surface of the central ganglia, and white profiles signify cells on the ventral surface. In the buccal ganglion, black cells are on the caudal surface and white cells are rostral. Neurons are not drawn to scale. Shading signifies nerves that are rich in THli fibers. Abbreviations: *A n.*: anal nerve, *A Pd n.*: anterior pedal nerve, *B g.*: buccal ganglion, *C-b c.*: cerebral-buccal connective, *C c.*: cerebral commissure, *Cer-pd c.*: cerebral-pedal connective, *Cer-Pl c.*: cerebral-pleural connective, *E Pa n.*: exterior parietal nerve, *E t.*: esophageal trunk, *I n.*: intestinal nerve, *I Pa n.*: interior parietal nerve, *Ld b.*: lateral-dorsal body *L Cer g.*: left cerebral ganglion, *L Pa g.*: left parietal ganglion, *LPdD1*: left pedal dorsal 1, *L Pd g.*: left pedal ganglion, *Md b.*: medial-dorsal body, *ML n.*: medial lip nerve, *M Pd n.*: middle pedal nerve, *P Pd n.:* posterior pedal nerve, *R Cer g.*: right cerebral ganglion, *R Pa g.*: right parietal ganglion, *R Pd g.*: right pedal ganglion, *R Pl g.*: right pleural ganglion, *SL n.*: superior lip nerve, *T n.*: tentacular nerve, *V g.*: visceral ganglion.